

Mechanical Properties of the Meninges: Large Language Model Assisted Systematic Review of over 25,000 Studies

January 31, 2024

Brandon P. Chelstrom¹, Maciej P. Polak², Dane Morgan², Corinne R. Henak^{1,3,4}

¹Department of Biomedical Engineering, University of Wisconsin-Madison, Madison, WI

²Department of Materials Science and Engineering, University of Wisconsin-Madison, Madison, WI

³Department of Mechanical Engineering, University of Wisconsin-Madison, Madison, WI

⁴Department of Orthopedics and Rehabilitation, University of Wisconsin-Madison, Madison, WI

*Address Correspondence to:

Corinne R. Henak, PhD
Associate Professor
3031 Mechanical Engineering Building
1513 University Ave
Madison, WI 53706
608-263-1619
chenak@wisc.edu

Word count: 5949 words

Keywords: Meninges, Mechanical Properties, Dura Mater, Arachnoid Mater, Pia Mater

The extracted data points from the modified ChatExtract were structured into a table and manually checked by a human reviewer (BPC) for relevance. A property triplet was deemed relevant if the passage corresponded to the correct material and included data from a primary mechanical study. Adhering to the central principle of the snowball search method, which uses the reference list of a relevant article as a starting point to find additional related studies, property triplets from referenced values were manually screened (Fig. 1). For studies confirmed to contain relevant information, a human reviewer (BPC) read the entire paper to extract all mechanical properties and associated categorical and numerical data. Categorical data included species, sex, sample location, sample orientation, and study-specific treatment. Numerical data included sample dimensions, donor or animal age, post-mortem time, post-mortem temperature, test temperature, loading rate, sample preconditioning, mechanical results, and constitutive model parameters. Sample location was split into two parts: whether the sample was spinal or cranial, and the anatomical location relative to either the spine or cortex. For numerical data, the average, standard deviation, minimum, maximum, and median values were collected when available. When possible, data was manually extracted from relevant figures, with priority given to values stated in the text. The collected data was structured for visualization in a custom MATLAB plotting tool called BioAxis Studio, to visualize various trends across relevant studies. Structured data for the *dura mater*, *arachnoid mater*, and *pia mater* and source code for the BioAxis Studio are available for download on Github (https://github.com/HenakLab/Brain_Interface).

Extracted categorical and numerical data were analyzed in three different stages beginning with patterns emerging for a single variable across multiple studies. Studies that did not report a relevant value were excluded from this analysis. Interesting trends that arose from at

Fig. 3. Effect of age on measured dura mater thickness in human (A) and porcine (B) samples show reverse trends, where thickness increases in human samples, but decreases in porcine samples with age.

3.1.3) Dura Mater Mechanical Properties

Qualitative trends between multiple variables were investigated using BioAxis Studio, and selected trends are highlighted here. Elastic modulus tended to increase with age for human cranial *dura mater*, ranging from 6.96 MPa for fetal tissue [67] to 62.6 MPa at 78.5 years [75] (Fig. 4A). Ultimate tensile stress and strain indicated an increasing ultimate tensile stress with age, from 1.57 MPa for fetal tissue [67] to 4.24 MPa at 78.5 years [75] (Fig. 4B), and a decreasing ultimate tensile strain, from 24% for fetal tissue [67] to 18% at 88 years [76] (Fig. 4C). No clear trend was visible for human spinal *dura mater* due to lack of data (Fig. 4A-C). However, porcine *dura mater* indicated three distinct sets of elastic moduli (Fig. 4D): spinal samples tested longitudinally (108.1 ± 40.3 MPa [71]), spinal samples tested transversely (53.2 ± 31.7 MPa [71]), and cranial samples (14.18 ± 2.48 MPa [77]).

For studies that fit an Ogden constitutive model, the Ogden stiffness ranged from -1.97 to 9.04 MPa and varied for location [78], orientation [79], and species [70] for some studies and not for others [64,70,71,80]. The Ogden exponentials for human tissue were generally negative (Fig.

S2), ranging from -94.33 to 65.56 and did not vary with location or orientation [80], while the Ogden exponentials for porcine tissue were generally positive (Fig. S2), ranging from 0.55 to 61.40 across multiple studies [64,70,71]. (Note that all Ogden parameters were transformed to a constant strain energy density prior to comparison, $W = \frac{\mu}{\alpha^2} (\lambda_1^\alpha + \lambda_2^\alpha + \lambda_3^\alpha)$, where μ is the stiffness, α is the exponential term, and λ_i are the principal stretches.)

The *dura mater* exhibits complex rate dependence for elastic modulus and ultimate tensile stress, which can be grouped into three distinct regions (Fig. S3). The spread of Elastic modulus and ultimate tensile stress initially increase from quasi-static loading rates (10 mm/min) to dynamic loading rates (150 mm/min), followed by an overall decrease in magnitude at higher dynamic rates (1500 mm/min). At extreme dynamic loading rates (18,000 mm/min – 42,000 mm/min), the elastic modulus and ultimate tensile stress drop significantly. As the rate further increases, the ultimate tensile stress remains relatively constant while the elastic modulus begins to increase (Fig. S3).

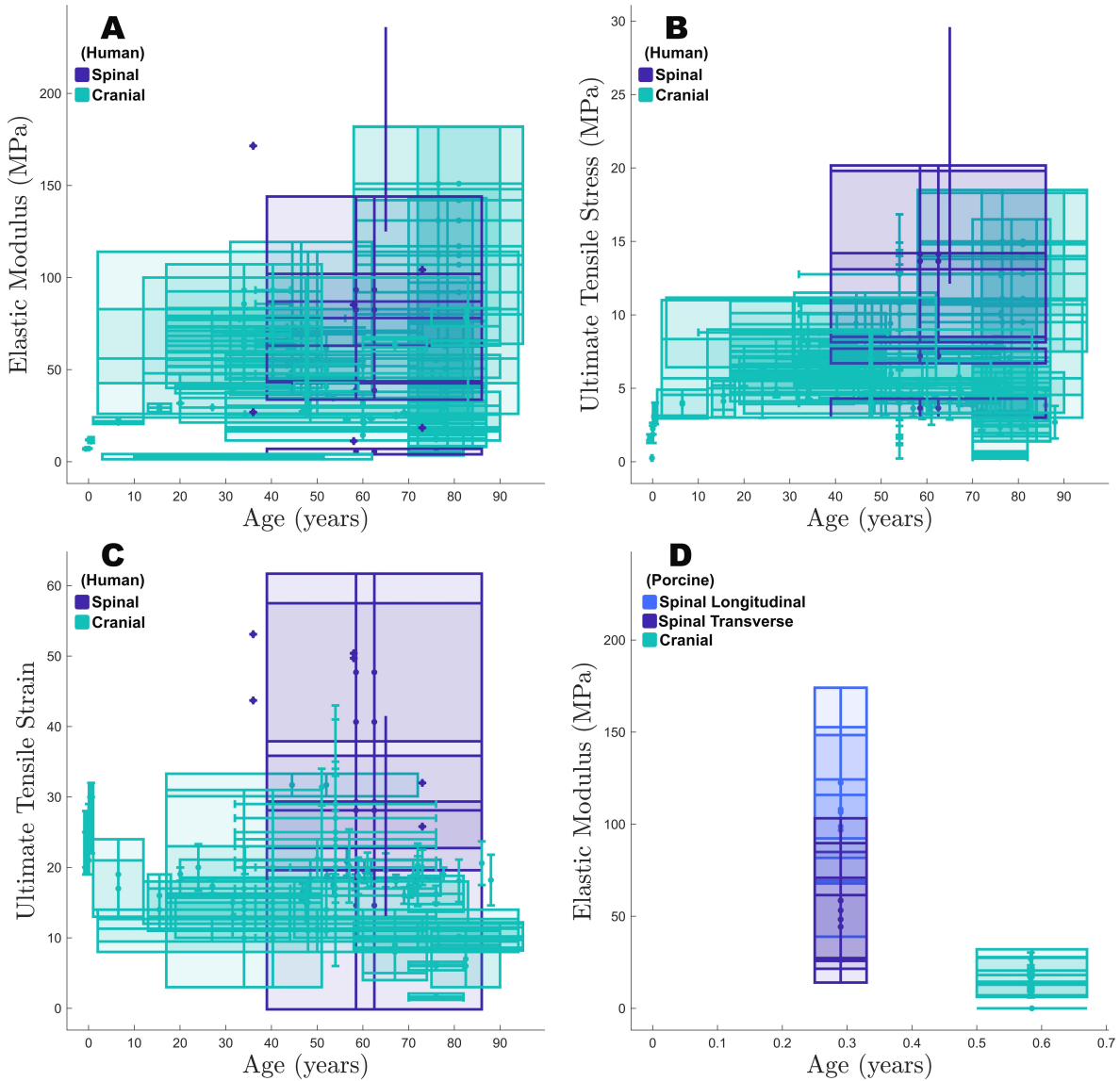


Fig. 4. Dura mater mechanical properties for human samples show the effect of age on modulus (A), ultimate strength (B), and ultimate strain (C). Porcine dura mater elastic modulus results include orientation effects in spinal samples (D).

3.2) Arachnoid Mater

3.2.1) Search Space Results

For the *arachnoid mater*, 1,816 studies were identified from the initial search filter across all 15 properties corresponding to over 230,000 passages (Fig. 1). ChatExtract identified 148 passages as potentially relevant, which removed 99.93% of the total search space. Following manual reclassification, 5 passages were deemed relevant corresponding to 4 primary mechanical

studies. Referenced values led to an additional 4 studies, resulting in 8 of the 1,816 studies ultimately included in this review. Only Walsh et al. reviewed the pia-arachnoid complex (PAC) which referred to both the *arachnoid mater* and *pia mater* [50]. This review identified all 5 studies related to the PAC found by Walsh et al., 4 of which were manually classified as *arachnoid mater* based on sample information provided in the methods [50]. Accounting for duplicate studies, this review identified 3 new studies related to *arachnoid mater* biomechanics, where 1 study was published after Walsh et al. [50].

3.1.2) Metadata: Study Characteristics and Reported Main Effects

Despite the small number of studies, study characteristics varied, and were often not tested statistically for the *arachnoid mater*. Studies were primarily performed on cranial tissue (7/8) and bovine tissue (4/8). Human tissue was only tested in 1 study. Due to the low number of studies, specific information on sample orientation (1/8), age (8/8), sex (3/8), post-mortem time (8/8), species (8/8), storage methods (8/8), test temperature/humidity (2/8), test hydration level (7/8), test type (8/8), and sample geometry (7/8) was often reported without testing its effect. Full details can be found in the *arachnoid mater* master table in the supplemental information (Table S3).

In contrast to the *dura mater*, sample storage was consistent across all 8 studies. Samples were stored in either a physiological salt solution (3/8) or artificial CSF (5/8) and were mostly tested without a freeze-thaw cycle (7/8), within either a 6-hour (3/8) or 56-hour (8/8) period. Studies were reported as testing immature (4/8), mature (3/8), or elderly (1/8) tissue samples, with ages not comparable across studies of different species. Species of test samples included bovine (4/8), ovine (1/8), porcine (1/8), rat (1/8), and human (1/8). Tissue thickness ranged from 20 μm to 53 μm for human [81], bovine [82–85], and rat [86] tissue samples, while ovine [87]

tissue samples ranged from 160 μm to 240 μm . Sex differences investigated for human tissue found no significant effect on tissue modulus, but found subject pair-wise differences for modulus, trabecular volume fraction, and membrane thickness [81]. Test methods included uniaxial tension (3/8), normal traction (2/8), uniaxial shear (2/8), atomic force microscopy (1/8), micro inflation (1/8), macro indentation (1/8), and micro indentation (1/8). Three studies used various constitutive models to fit mechanical data including a fiber reinforced viscoelastic Mooney-Rivlin [84], Maxwell and Ogden [86], and elastic thin-substrate constitutive models [88].

3.1.3) Arachnoid Mater *Mechanical Properties*

Any apparent effect of sample storage, post-mortem time, or sample age were overshadowed by differences between species (Fig. 5). Bovine *arachnoid mater* had the highest traction modulus [82,83,85], followed by porcine [88], human [81], and rat [86], which tended to scale with species body mass (Fig. 5). A power law fit to data averages resulted in an exponent of 0.54 with an R^2 of 0.957 and root mean square error normalized by the range of 7.54%. Related to tissue thickness, the volume fraction of trabeculae within the subarachnoid space varies considerably across the surface of the brain, leading to heterogenous mechanical properties for the *arachnoid mater* [81,86].

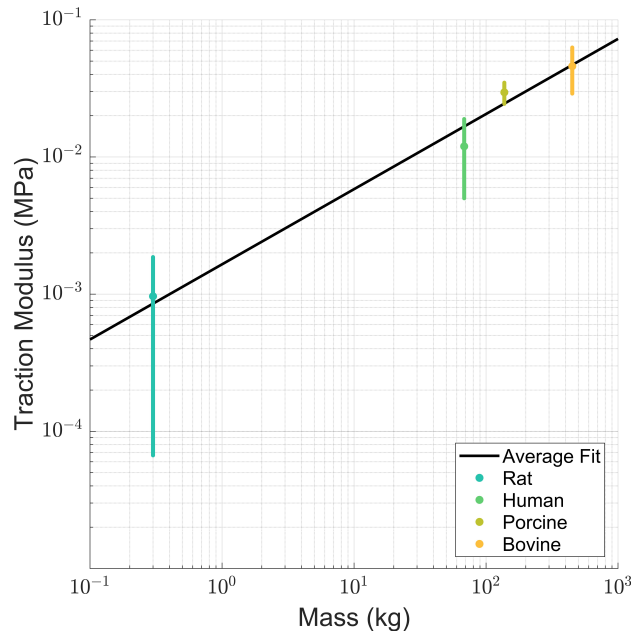


Fig. 5: Arachnoid mater traction modulus across species as a function of body mass (Rat [89], Human [89], Porcine [90], Bovine [89]). The black line was directly fit to the four data averages which indicates a proportional increase in traction modulus with body size $Traction\ Modulus = 0.00164 * Mass^{0.547}$ with an R^2 of 0.957 and normalized root mean square error of 7.83%.

3.3) Pia Mater

3.2.1) Search Space Results

For the *pia mater*, 5,654 studies were identified from the initial search filter across all 15 properties leading to over 600,000 passages (Fig. 1). ChatExtract deemed 375 passages as possibly relevant, removing 99.94% of the total search space. Through manual review, 12 passages corresponding to 3 primary mechanical papers were included. Tracing referenced values led to an additional 4 studies, resulting in 7 of the original 5,654 studies ultimately included in the review. Of the 5 studies found by Walsh et al. for the PAC, only 1 was classified as testing the *pia mater* for this review while the other 4 studies were classified as testing the *arachnoid mater* [50]. Accounting for duplicates, this review found 6 additional primary mechanical studies related to *pia mater* biomechanics, where 1 was published after Walsh et al. [50].

3.1.2) Metadata: Study Characteristics and Reported Main Effects

Pia mater studies were tested exclusively in non-human samples. Other study characteristics were variable between studies. Studies were primarily performed on spinal tissue (5/7). While there was no human tissue, canine (1/7), bovine (1/7), ovine (1/7), lapine (1/7) and porcine *pia mater* (3/7) were tested. Specific information on sample orientation (4/7), age (4/7), sex (1/7), post-mortem time (7/7), species (7/7), storage methods (7/7), test temperature/humidity (5/7), test hydration level (7/7), test type (7/7), and sample geometry (7/7) were reported but not statistically evaluated. Full details can be found in the *pia mater* master table in the supplemental information (Table S4).

Similar to the *arachnoid mater*, sample storage for the *pia mater* was consistent across all relevant studies. Most studies stored samples in physiological salt solutions (7/8) between temperatures of 4°C to 24°C (5/7) and tested samples 16 hours post-mortem (7/7). Sample age varied with species, which were porcine (3/7), dog (1/7), lapine (1/7), bovine (1/7), and ovine (1/7), and were classified as immature (2/4) or mature (2/4). Significant effects of sample storage, post-mortem time, and sample age could not be investigated between species due to the low number of identified studies. Tissue thickness was reported in 3 studies, with ovine [28] ranging from 4.14 μm to 5.78 μm , rabbit [91] ranging from 9 μm to 15 μm , and porcine [92] ranging from 110 μm to 330 μm . Sex was only reported in one study [92], but its effects were not analyzed. Sample orientation was reported in 4 studies, 2 of which were on porcine spinal samples which found a higher elastic modulus and ultimate tensile strength in the longitudinal direction compared to the transverse direction [71,92]. The other 2 studies were only tested in one direction on different species [91,93]. Sample orientation was not investigated for cranial samples. Test methods included uniaxial tension (4/7), creep (2/7), biaxial (1/7), and stress relaxation (1/7). Various constitutive models were used to fit experimental data in five studies

including a one term Ogden model [28,71,92] (3/5), neo-Hookean model [94] (1/5), and both isotropic and anisotropic Gasser-Ogden-Holzapfel (GOH) and Gasser models [71] (1/5).

3.1.3) Pia Mater Mechanical Properties

Because of the sparsity of reported data, trends were challenging to observe. The effect of sample thickness and species on mechanical properties could only be partially investigated based on reported data. Porcine [71,92,94] *pia mater* was the thickest and had the highest elastic modulus followed by lapine [91] and ovine [28] (Fig. 6A). Ultimate tensile stress tended to increase with ultimate tensile strain independent of species [28,71,92,94] (Fig. 6B). *Pia mater* behavior is nonlinear, with the elastic modulus increasing with strain rate [28,94] and strain [28,71,92,94].

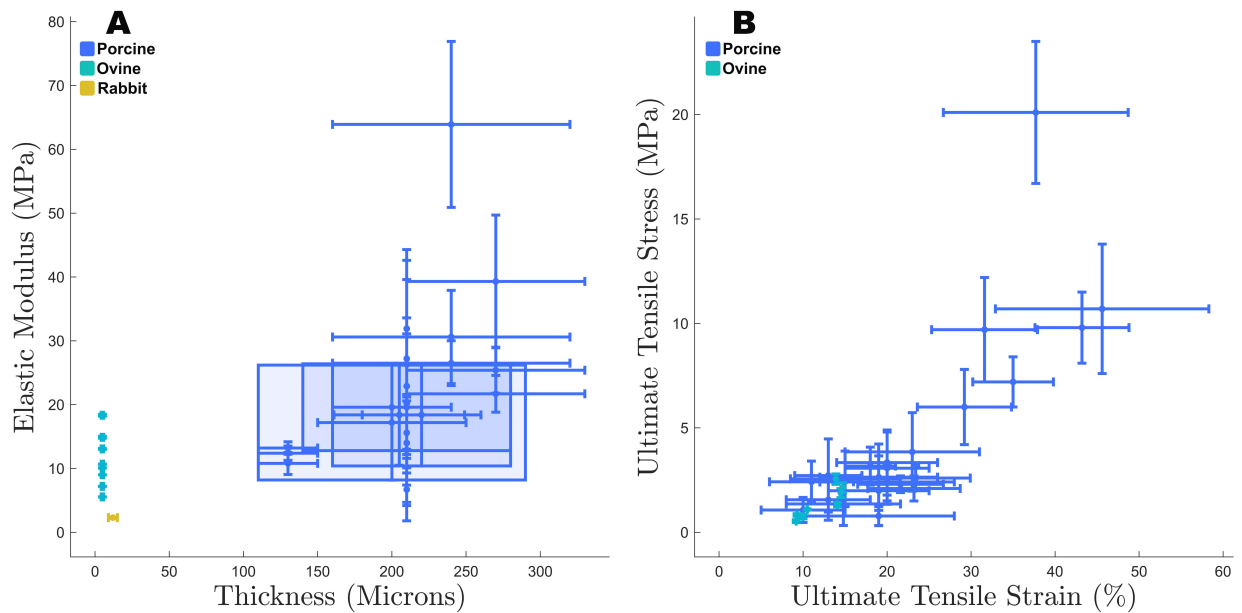


Fig. 6: Pia mater thickness and elastic modulus across species (A), and ultimate tensile strain and ultimate tensile stress across species (B).

4) Discussion

In this study, we conducted an LLM-assisted SR on the mechanical properties of the meninges. Each layer of the meninges was reviewed independently scanning 17,951 studies for the *dura mater*, 1,816 studies for the *arachnoid mater*, and 5,654 studies for the *pia mater*. Primary

mechanical studies on meningeal mechanics were identified through a combination of an automated and manual review process resulting in 47 studies for the *dura mater*, 8 studies for the *arachnoid mater*, and 7 studies for the *pia mater*. Accounting for duplicates, this review identified 28 previously unreviewed studies related to *dura mater* mechanics, 3 studies related to *arachnoid mater* mechanics, and 6 studies related to *pia mater* mechanics.

Mechanical properties of biological tissues vary widely due to biological variation between species, anatomical locations, and individuals. The most notable source of variation for the meninges came from differences between species (e.g., bovine [82], human [27], ovine [28], porcine [71], rabbit [91], and rat [86]). Variation in sample location, such as cranial tissue [28,73,81,95], spinal tissue [71,87,96], as well as anatomical location [43,70,71,77,81,82,87,97,98], contributed to variability as well. Tissue was most often tested in uniaxial tension, which commonly corresponded to reporting bulk elastic modulus, ultimate tensile strain, and ultimate tensile stress. The reported mechanical properties for the *dura* and *pia mater* are most similar to soft elastomers such as silicon, rubber, and other biological materials such as ligament and cartilage (Fig. 2). The *arachnoid mater* is noticeably softer and weaker than other biological materials and common synthetic hydrogels (Fig. 2). Material guidelines suggest similar elastic energy storage for the *dura mater* and *pia mater* with lower elastic energy storage for the *arachnoid mater*, but similar yield strains for each layer (Fig. 2). Compared to other materials, the meninges have comparable elastic energy storage to most engineered or hard materials with high yield strains most similar to synthetic elastomers (Fig. 2). While linear tissue properties are well reported [26,49,66,77], there remains a dearth of information on the nonlinear mechanical behavior, particularly for the *arachnoid* and *pia mater*. Descriptive mechanical studies investigating failure behavior and a wide range of loading rates are lacking; the effect of

sample-specific factors such as age, sex, species, storage methods, and environmental test levels are similarly under reported. Reporting age in tandem with species is of critical importance for comparing animal models because different species age and mature at different rates. To best fill these gaps in the current literature, future studies should state species, sample location, sample orientation, sample treatment, sex, and any preconditioning and fully report mean, standard deviation, and range for age, post-mortem time, loading rate, sample length, sample width, and sample thickness.

The *dura mater* has been the most extensively studied meningeal tissue, and exhibits nonlinear [77], rate-dependent [42], viscoelastic [44] mechanical behavior, which is locally anisotropic and heterogenous in the skull [41,75], globally isotropic and homogenous in the skull [77,80], and globally anisotropic and heterogenous in the spine [71,92]. The most commonly reported constitutive models are a one term viscoelastic Ogden model for cranial tissue [64,80,95], and a viscoelastic GOH model, which considers longitudinal and transverse fiber orientations, for spinal tissue [71,75]. Specific model parameters vary significantly for species, age, and loading rate which require extra consideration when selecting constitutive model parameters for FE modeling. When possible, mechanical analysis should be conducted on human tissue hydrated in a physiological saline solution at body temperature [64,71,75,79,94]. In place of human tissue, the most commonly used animal model has been mature porcine tissue [43,64,70–74,77,96,98–100] as it most closely matches the *dura mater* thickness and elastic modulus (Fig. 3, 4A, 4D) as well as exhibiting similar lipid content [101,102], DNA polymerase [101–103], and water content [101] to human tissue during development [104]. Still unknown are the effects of tissue hydration post-mortem, dynamic loading rates (1000 – 100,000

mm/min), how relative age between species impacts tissue animal models, the transition point for isotropy and homogeneity for cranial tissue, and interactions between adjacent tissues.

Considerably less information exists on the mechanical properties for the *arachnoid* and *pia mater* compared to the *dura mater*. Bovine *arachnoid mater* has been extensively studied and modeled using a homogenous nonlinear, rate-dependent, viscoelastic constitutive model [82–85] but is considerably stiffer compared to other species including human tissue (Fig. 5).

Additionally, this model did not consider structural nonlinearity arising from the multiple loading regimes of individual sub-arachnoid trabeculae [27], or the heterogeneity with respect to the skull [27,40]. Of all animal models reported, porcine tissue most closely resembled the elastic modulus [88] and thickness [88] of human *arachnoid mater* (Fig. 5), though it has a higher volume fraction of sub arachnoid trabeculae [39,40]. Anatomical studies [30,32,105] suggest that testing the *arachnoid* in isolation from the *pia* is an arduous task due to the anchoring of the subarachnoid trabeculae in the *pia mater*. Future studies on the mechanical properties of the *arachnoid mater* should be conducted on hydrated human or porcine tissue with the *pia mater* intact. Studies on human *pia mater* were not found in this review, and spinal and cranial *pia mater* has not been tested with in the same species. Constitutive models fit to *pia mater* experimental data found loading rate dependent [28,94], nonlinear [106], viscoelastic [93] behavior that varies in direction and location along the spine [71,92]. The *pia mater* can be tested in isolation from the *arachnoid mater*; however, a process for isolating the *pia mater* from the *arachnoid mater* without damage is still unknown. Current FE head models often use a simplified linear elastic constitutive model for the *pia mater* with a modulus of 2.3 MPa [91]; however, multiple studies in this review have reported elastic moduli an order of magnitude higher in both the longitudinal (~ 20 MPa) and transverse (~10 MPa) directions [28,71,92] (Fig.

6A). Future studies should investigate how species, age, sex, loading rate, post-mortem time, and tissue hydration affect the complex mechanical behavior of the *pia mater*.

The semi-automatic approach to a literature review required less time to process a larger number of studies. While exact hours were not tracked, the manual portion of the review took between 600 - 680 hours to complete (corresponding to 15 - 17 standard 40-hr work weeks) to review over 25,000 studies. A standard SR which averages 4.34 studies per person hour (881 person-hours to review 3781 studies [54]) would require over 100,000 hours to review the same 25,000 studies. While this review included a much larger breadth of studies compared to a standard SR, there are some limitations in this analysis. Only full text studies from ScienceDirect that were open source or available under the UW-Madison license were considered. The majority of studies (>99.9%) were automatically scanned using a conversational LLM where it is difficult to know what factors were considered when reviewing studies. Manual evaluation was only applied after automatic classification, which could have led to the rejection of some relevant studies without the reviewer's knowledge. This effect was minimized by using a combination of general and specific search terms which was shown to have different levels of precision and recall (Fig. S1). The automatic portion of the review required access to considerable computational resources or a paid access to the LLM as a service. Additionally, only a single reviewer (BPC) analyzed the results, which could lead to bias in data extraction, classification, and relevancy.

Current FE head models often neglect or oversimplify the mechanical properties of the meninges, which can drastically influence prediction accuracy. This study conducted a semi-automatic systematic review of the mechanical properties of the meninges using a modified ChatExtract algorithm and a single human reviewer. Over 25,000 papers (~2.6 million passages)

were considered where 47 studies related to the *dura mater*, 8 studies related to the *arachnoid mater*, and 7 studies related to the *pia mater* were ultimately included. All three layers of the meninges were found to be rate dependent, nonlinear viscoelastic and individually vary with respect to species, age, location, and orientation. Future FE head models that use a linear elastic constitutive model for the *pia mater* should use an order of magnitude higher elastic modulus compared to previous FE models. Studies on the interaction between different meningeal layers were sparse which could lead to inaccurate modeling of tissue boundaries even with accurate constitutive models. Future research on meningeal mechanical properties should primarily investigate a broader spectrum of quasi-static and dynamic loading rates, considering both the presence and absence of age-related effects on the *arachnoid* and *pia mater*, as these factors are anticipated to influence the accuracy of finite element (FE) predictions.

5) Acknowledgements

We gratefully acknowledge support from the Office of Naval Research via the PANTHER program under Dr. Timothy Bentley (N00014-23-1-2825). This project would not have been possible without the technical and administrative support provided by librarian Dave Bloom in database selection and review methodology as well as Nolan Thole for LLM and search term validation. Their efforts were crucial to handling such a large number of studies and for a smooth execution of this project.

6) Declaration of Competing Interest

The authors declare that they have no known competing financial interests or personal relationships that could have appeared to influence the work reported in this paper.

7) CRediT authorship contribution statement

Brandon P. Chelstrom: Methodology, Software, Validation, Investigation, Data Curation,
Writing – Original Draft, Review, & Editing, Visualization **Maciej P. Polak:** Methodology,
Software, Validation, Writing – Original Draft, Review, & Editing **Dane Morgan:**
Conceptualization, Funding Acquisition, Writing – Review, & Editing **Corinne R. Henak:**
Conceptualization, Resources, Writing – Review, & Editing, Supervision, Funding Acquisition

8) References

- [1] J. Daugherty, D. Waltzman, K. Sarmiento, L. Xu, Morbidity and Mortality Weekly Report Traumatic Brain Injury-Related Deaths by Race/Ethnicity, Sex, Intent, and Mechanism of Injury-United States, 2000-2017, 2019. <https://www.cdc.gov/nchs/products/databriefs/db328.htm>.
- [2] J. Daugherty, K. Sarmiento, D. Waltzman, L. Xu, Traumatic Brain Injury–Related Hospitalizations and Deaths in Urban and Rural Counties—2017, *Ann Emerg Med* 79 (2022) 288-296.e1. <https://doi.org/10.1016/j.annemergmed.2021.09.433>.
- [3] J.A. Langlois, W. Rutland-Brown, M.M. Wald, The Epidemiology and Impact of Traumatic Brain Injury A Brief Overview, *J Head Trauma Rehabil* 21 (2006) 375–378. <http://journals.lww.com/headtraumarehab>.
- [4] D. Thurman, C. Alverson, D. Browne, K. Dunn, J. Guerrero, R. Johnson, V. Johnson, J. Langlois, D. Pilkey, J. Sniezek, S. Toal, P. Gosler, B. Gabella, R. Hoffman, G. Whieneck, M. Kinde, J. Roesler, G. Land, M. Tuinen, L. Santilli, K. Thoburn, G. Feck, P. Archer, M. Crutcher, S. Mallonee, E. McCutcheon, A. Selassie, L. Frazier, Traumatic Brain Injury in the United States: A Report to Congress, 1999.
- [5] The Management and Rehabilitation of Post-Acute Mild Traumatic Brain Injury Work Group, VA/DoD Clinical Practice Guideline for the Management and Rehabilitation of Post-Acute Mild Traumatic Brain Injury, 2021. www.tricare.mil.
- [6] S.M. Slobounov, A. Walter, H.C. Breiter, D.C. Zhu, X. Bai, T. Bream, P. Seidenberg, X. Mao, B. Johnson, T.M. Talavage, The effect of repetitive subconcussive collisions on brain integrity in collegiate football players over a single football season A multi-modal neuroimaging study, *Neuroimage Clin* 14 (2017) 708–718. <https://doi.org/10.1016/j.nicl.2017.03.006>.
- [7] T.M. Talavage, E.A. Nauman, E.L. Breedlove, U. Yoruk, A.E. Dye, K.E. Morigaki, H. Feuer, L.J. Leverenz, Functionally-detected cognitive impairment in high school football players without clinically-diagnosed concussion, *J Neurotrauma* 31 (2014) 327–338. <https://doi.org/10.1089/neu.2010.1512>.
- [8] S. Parikh, M. Koch, R.K. Narayan, Traumatic Brain Injury, *Int Anesthesiol Clin* 45 (2007) 119–135. <http://journals.lww.com/anesthesiaclinics>.
- [9] A.G. Kolias, P.J. Kirkpatrick, P.J. Hutchinson, Decompressive craniectomy: past, present and future, *Nat Rev Neurol* 9 (2013) 405–415. <https://doi.org/10.1038/nrneurol.2013.106>.
- [10] J.S. Giudice, W. Zeng, T. Wu, A. Alshareef, D.F. Shedd, M.B. Panzer, An Analytical Review of the Numerical Methods used for Finite Element Modeling of Traumatic Brain Injury, *Ann Biomed Eng* 47 (2019) 1855–1872. <https://doi.org/10.1007/s10439-018-02161-5>.
- [11] N.G. Ibrahim, R. Natesh, S.E. Szczesny, K. Ryall, S.A. Eucker, B. Coats, S.S. Margulies, In situ deformations in the immature brain during rapid rotations, *J Biomech Eng* 132 (2010). <https://doi.org/10.1115/1.4000956>.
- [12] R.W. Carlsen, A.L. Fawzi, Y. Wan, H. Kesari, C. Franck, A quantitative relationship between rotational head kinematics and brain tissue strain from a 2-D parametric finite element analysis, *Brain Multiphys* 2 (2021). <https://doi.org/10.1016/j.brain.2021.100024>.
- [13] N.C. Colgan, M.D. Gilchrist, K.M. Curran, Applying DTI white matter orientations to finite element head models to examine diffuse TBI under high rotational accelerations,

- Prog Biophys Mol Biol 103 (2010) 304–309.
<https://doi.org/10.1016/j.pbiomolbio.2010.09.008>.
- [14] B. Coats, G. Binenbaum, C. Smith, R.L. Peiffer, C.W. Christian, A.C. Duhaime, S.S. Margulies, Cyclic head rotations produce modest brain injury in infant piglets, *J Neurotrauma* 34 (2017) 235–247. <https://doi.org/10.1089/neu.2015.4352>.
- [15] A. Al-Bsharat, W. Hardy, K. Yang, T. Khalil, Brain/Skull Relative Displacement Magnitude Due to Blunt Head Impact: New Experimental Data and Model, *Stamp Car Crash Conference Proceedings* (1999) 321–331.
- [16] K.A. Kailash, C.A. Guertler, C.L. Johnson, R.J. Okamoto, P. V. Bayly, Measurement of relative motion of the brain and skull in the mini-pig in-vivo, *J Biomech* 156 (2023). <https://doi.org/10.1016/j.jbiomech.2023.111676>.
- [17] A.A. Badachhape, R.J. Okamoto, R.S. Durham, B.D. Efron, S.J. Nadell, C.L. Johnson, P. V. Bayly, The Relationship of Three-Dimensional Human Skull Motion to Brain Tissue Deformation in Magnetic Resonance Elastography Studies, *J Biomech Eng* 139 (2017). <https://doi.org/10.1115/1.4036146>.
- [18] M.M. Mortazavi, S.A. Quadri, M.A. Khan, A. Gustin, S.S. Suriya, T. Hassanzadeh, K.M. Fahimdanesh, F.H. Adl, S.A. Fard, M.A. Taqi, I. Armstrong, B.A. Martin, R.S. Tubbs, Subarachnoid Trabeculae: A Comprehensive Review of Their Embryology, Histology, Morphology, and Surgical Significance, *World Neurosurg* 111 (2018) 279–290. <https://doi.org/10.1016/j.wneu.2017.12.041>.
- [19] G.G. Scott, S.S. Margulies, B. Coats, Utilizing multiple scale models to improve predictions of extra-axial hemorrhage in the immature piglet, *Biomech Model Mechanobiol* 15 (2016) 1101–1119. <https://doi.org/10.1007/s10237-015-0747-0>.
- [20] S. Yang, J. Tang, B. Nie, Q. Zhou, Assessment of brain injury characterization and influence of modeling approaches, *Sci Rep* 12 (2022). <https://doi.org/10.1038/s41598-022-16713-2>.
- [21] S. Sullivan, S.A. Eucker, D. Gabrieli, C. Bradfield, B. Coats, M.R. Maltese, J. Lee, C. Smith, S.S. Margulies, White matter tract-oriented deformation predicts traumatic axonal brain injury and reveals rotational direction-specific vulnerabilities, *Biomech Model Mechanobiol* 14 (2015) 877–896. <https://doi.org/10.1007/s10237-014-0643-z>.
- [22] L. Zhang, K.H. Yang, A.I. King, A Proposed Injury Threshold for Mild Traumatic Brain Injury, *J Biomech Eng* 126 (2004) 226–236. <https://doi.org/10.1115/1.1691446>.
- [23] E. Bar-Kochba, M.T. Scimone, J.B. Estrada, C. Franck, Strain and rate-dependent neuronal injury in a 3D in vitro compression model of traumatic brain injury, *Sci Rep* 6 (2016). <https://doi.org/10.1038/srep30550>.
- [24] H. Gray, P. Williams, L. Bannister, *Gray's anatomy*, 38th ed., Churchill Livingstone, Edinburgh, 1995.
- [25] F. Herisson, V. Frodermann, G. Courties, D. Rohde, Y. Sun, K. Vandoorne, G.R. Wojtkiewicz, G.S. Masson, C. Vinegoni, J. Kim, D.E. Kim, R. Weissleder, F.K. Swirski, M.A. Moskowitz, M. Nahrendorf, Direct vascular channels connect skull bone marrow and the brain surface enabling myeloid cell migration, *Nat Neurosci* 21 (2018) 1209–1217. <https://doi.org/10.1038/s41593-018-0213-2>.
- [26] J. Zwirner, M. Scholze, J.N. Waddell, B. Ondruschka, N. Hammer, Mechanical Properties of Human Dura Mater in Tension – An Analysis at an Age Range of 2 to 94 Years, *Sci Rep* 9 (2019). <https://doi.org/10.1038/s41598-019-52836-9>.

- [27] N. Benko, E. Luke, Y. Alsanea, B. Coats, Mechanical characterization of the human pia-arachnoid complex, *J Mech Behav Biomed Mater* 120 (2021). <https://doi.org/10.1016/j.jmbbm.2021.104579>.
- [28] Y. Li, W. Zhang, Y.C. Lu, C.W. Wu, Hyper-viscoelastic mechanical behavior of cranial pia mater in tension, *Clinical Biomechanics* 80 (2020). <https://doi.org/10.1016/j.clinbiomech.2020.105108>.
- [29] F. Vandenabeele, J. Creemers, I. Lambrechts, Ultrastructure of the human spinal arachnoid mater and dura mater, *J. Anat* 189 (1996) 417–430.
- [30] R.O. Weller, Microscopic morphology and histology of the human meninges, *Morphologie* 89 (2005) 22–34. [https://doi.org/10.1016/S1286-0115\(05\)83235-7](https://doi.org/10.1016/S1286-0115(05)83235-7).
- [31] R. Alcolado, R.O. Weller, P. Parrish, D. Garrod, The Cranial Arachnoid and Pia Mater in Man: Anatomical and Ultrastructural Observations, *Neuropathol Appl Neurobiol* 14 (1988) 1–17. <https://doi.org/10.1111/j.1365-2990.1988.tb00862.x>.
- [32] P. Saboori, A. Sadegh, Histology and Morphology of the Brain Subarachnoid Trabeculae, *Anat Res Int* 2015 (2015) 1–9. <https://doi.org/10.1155/2015/279814>.
- [33] C.W. Kerber, T.H. Newton, The Macro and Microvasculature of the Dura Mater*, *Neuroradiology* 6 (1973) 175–179.
- [34] M. Protasoni, S. Sangiorgi, A. Cividini, G.T. Culuvaris, G. Tomei, C. Dell’Orbo, M. Raspanti, S. Balbi, M. Reguzzoni, The collagenic architecture of human dura mater: Laboratory investigation, *J Neurosurg* 114 (2011) 1723–1730. <https://doi.org/10.3171/2010.12.JNS101732>.
- [35] W. Schachenmayr, R.L. Friede, The Origin of Subdural Neomembranes I. Fine Structure of the Dura-Arachnoid Interface in Man, *American Journal of Pathology* (1978) 53–62.
- [36] N. Adeeb, M.M. Mortazavi, R.S. Tubbs, A.A. Cohen-Gadol, The cranial dura mater: A review of its history, embryology, and anatomy, *Child’s Nervous System* 28 (2012) 827–837. <https://doi.org/10.1007/s00381-012-1744-6>.
- [37] N. Adeeb, M.M. Mortazavi, A. Deep, C.J. Griessenauer, K. Watanabe, M.M. Shoja, M. Loukas, R.S. Tubbs, The pia mater: A comprehensive review of literature, *Child’s Nervous System* 29 (2013) 1803–1810. <https://doi.org/10.1007/s00381-013-2044-5>.
- [38] A. Kinaci, W. Bergmann, R.L.A.W. Bleys, A. van der Zwan, T.P.C. van Doormaal, Histologic comparison of the dura mater among species, *Comp Med* 70 (2020) 170–175. <https://doi.org/10.30802/AALAS-CM-19-000022>.
- [39] G.G. Scott, B. Coats, Microstructural Characterization of the Pia-Arachnoid Complex Using Optical Coherence Tomography, *IEEE Trans Med Imaging* 34 (2015) 1452–1459. <https://doi.org/10.1109/TMI.2015.2396527>.
- [40] N. Benko, E. Luke, Y. Alsanea, B. Coats, Spatial distribution of human arachnoid trabeculae, *J Anat* 237 (2020) 275–284. <https://doi.org/10.1111/joa.13186>.
- [41] M.S. Sacks, J. Hamann, S.E. Otano-Lata, T.I. Malinin, Local Mechanical Anisotropy in Human Cranial Dura Mater Allografts, *J Biomech Eng* 120 (1998) 541–544. http://asmedigitalcollection.asme.org/biomechanical/article-pdf/120/4/541/5767037/541_1.pdf.
- [42] J. Zwirner, B. Ondruschka, M. Scholze, A. Thambyah, J. Workman, N. Hammer, J.A. Niestrawska, Dynamic load response of human dura mater at different velocities, *J Mech Behav Biomed Mater* 138 (2023). <https://doi.org/10.1016/j.jmbbm.2022.105617>.

- [43] E. Mazgajczyk, K. Scigala, M. Czy, W. Jarmundowicz, R. BedZinski, Mechanical Properties of Cervical Dura Mater, *Acta of Bioengineering and Biomaterials* 14 (2012) 51–58.
- [44] J. Galford E., J. McElhaney H., A Viscoelastic Study of Scalp, Brain, and Dura, *J Biomech* 3 (1970) 211–221. [https://doi.org/10.1016/0021-9290\(70\)90007-2](https://doi.org/10.1016/0021-9290(70)90007-2).
- [45] R.K. Wilcox, L.E. Bilston, D.C. Barton, R.M. Hall, Mathematical model for the viscoelastic properties of dura mater, in: *J Orthop Sci*, 2003: pp. 432–434.
- [46] L. Gu, M.S. Chafi, S. Ganpule, N. Chandra, The influence of heterogeneous meninges on the brain mechanics under primary blast loading, *Compos B Eng* 43 (2012) 3160–3166. <https://doi.org/10.1016/j.compositesb.2012.04.014>.
- [47] A. Madhukar, M. Ostoja-Starzewski, Finite Element Methods in Human Head Impact Simulations: A Review, *Ann Biomed Eng* 47 (2019) 1832–1854. <https://doi.org/10.1007/s10439-019-02205-4>.
- [48] K. Ming Tse, H. Lee, S. Piang Lim, V. Beng Chye Tan, H. Pueh Lee, H.A. Pueh Lee, A Review of Head Injury and Finite Element Head Models, *American Journal of Engineering, Technology, and Society* 1 (2014) 28–52. <http://www.openscienceonline.com/journal/ajets>.
- [49] Q. Percy, J. Tomlinson, J.A. Niestrawska, D. Möbius, M. Zhang, J. Zwirner, Systematic review and meta-analysis of the biomechanical properties of the human dura mater applicable in computational human head models, *Biomech Model Mechanobiol* 21 (2022) 755–770. <https://doi.org/10.1007/s10237-022-01566-5>.
- [50] D.R. Walsh, Z. Zhou, X. Li, J. Kearns, D.T. Newport, J.J.E. Mulvihill, Mechanical Properties of the Cranial Meninges: A Systematic Review, *J Neurotrauma* 38 (2021) 1748–1761. <https://doi.org/10.1089/neu.2020.7288>.
- [51] M.J. Page, J.E. McKenzie, P.M. Bossuyt, I. Boutron, T.C. Hoffmann, C.D. Mulrow, L. Shamseer, J.M. Tetzlaff, E.A. Akl, S.E. Brennan, R. Chou, J. Glanville, J.M. Grimshaw, A. Hróbjartsson, M.M. Lalu, T. Li, E.W. Loder, E. Mayo-Wilson, S. McDonald, L.A. McGuinness, L.A. Stewart, J. Thomas, A.C. Tricco, V.A. Welch, P. Whiting, D. Moher, The PRISMA 2020 statement: An updated guideline for reporting systematic reviews, *The BMJ* 372 (2021). <https://doi.org/10.1136/bmj.n71>.
- [52] R.A. Damarell, N. May, S. Hammond, R.M. Sladek, J.J. Tieman, Topic search filters: a systematic scoping review, *Health Info Libr J* 36 (2019) 4–40. <https://doi.org/10.1111/hir.12244>.
- [53] V.J. White, J.M. Glanville, C. Lefebvre, T.A. Sheldon, A statistical approach to designing search filters to find systematic reviews: objectivity enhances accuracy, *J Inf Sci* (2001). <https://doi.org/https://doi.org/10.1177/016555150102700601>.
- [54] B. Pham, E. Bagheri, P. Rios, A. Pourmasoumi, R.C. Robson, J. Hwee, W. Isaranuwatjai, N. Darvesh, M.J. Page, A.C. Tricco, Improving the conduct of systematic reviews: a process mining perspective, *J Clin Epidemiol* 103 (2018) 101–111. <https://doi.org/10.1016/j.jclinepi.2018.06.011>.
- [55] L. Bornmann, R. Haunschild, R. Mutz, Growth rates of modern science: a latent piecewise growth curve approach to model publication numbers from established and new literature databases, *Humanit Soc Sci Commun* 8 (2021). <https://doi.org/10.1057/s41599-021-00903-w>.

- [56] S.R. Jonnalagadda, P. Goyal, M.D. Huffman, Automating data extraction in systematic reviews: A systematic review, *Syst Rev* 4 (2015). <https://doi.org/10.1186/s13643-015-0066-7>.
- [57] H. Khalil, D. Ameen, A. Zarnegar, Tools to support the automation of systematic reviews: a scoping review, *J Clin Epidemiol* 144 (2022) 22–42. <https://doi.org/10.1016/j.jclinepi.2021.12.005>.
- [58] Q. Khraisha, S. Put, J. Kappenberg, A. Warraitch, K. Hadfield, Can large language models replace humans in systematic reviews? Evaluating GPT-4's efficacy in screening and extracting data from peer-reviewed and grey literature in multiple languages, *Res Synth Methods* (2024). <https://doi.org/10.1002/jrsm.1715>.
- [59] M.P. Polak, S. Modi, A. Latosinska, J. Zhang, C.W. Wang, S. Wang, A.D. Hazra, D. Morgan, Flexible, model-agnostic method for materials data extraction from text using general purpose language models, *Digital Discovery* 3 (2024) 1221–1235. <https://doi.org/10.1039/d4dd00016a>.
- [60] M.P. Polak, D. Morgan, Extracting Accurate Materials Data from Research Papers with Conversational Language Models and Prompt Engineering, (2023). <http://arxiv.org/abs/2303.05352>.
- [61] A. Li, Y. Si, X. Wang, X. Jia, X. Guo, Y. Xu, Poly(vinyl alcohol) Nanocrystal-Assisted Hydrogels with High Toughness and Elastic Modulus for Three-Dimensional Printing, *ACS Appl Nano Mater* 2 (2019) 707–715. <https://doi.org/10.1021/acsanm.8b01786>.
- [62] M. Ashby F., *Materials Selection in Mechanical Design*, 5th ed., Todd Green, 2016.
- [63] J. Exton, J.M.G. Higgins, J. Chen, Acute brain slice elastic modulus decreases over time, *Sci Rep* 13 (2023) 12826. <https://doi.org/10.1038/s41598-023-40074-z>.
- [64] B. Pierrat, L. Carroll, F. Merle, D.B. MacManus, R. Gaul, C. Lally, M.D. Gilchrist, A. Ní Annaidh, Mechanical Characterization and Modeling of the Porcine Cerebral Meninges, *Front Bioeng Biotechnol* 8 (2020). <https://doi.org/10.3389/fbioe.2020.00801>.
- [65] R. Van Noort, T.R.P. Martin, M.M. Black, A.T. Barker, C.G. Montero, The mechanical properties of human dura mater and the effects of storage media, *Clin. Phys. Physiol. Meas* 2 (1981) 197–203. <https://doi.org/https://doi.org/10.1088/0143-0815/2/3/003>.
- [66] R. Van Noort, M.M. Black, T.R.P. Martin, S. Meanley, A study of the uniaxial mechanical properties of human dura mater preserved in glycerol, 1980.
- [67] V.I. Zyablov, Y.N. Shapovalov, K.D. Toskin, V. V Tkach, V. V Zhebrovsky, L.S. Georgievskaya, Structure and Physical-Mechanical Properties of the Human Dural Mind in the Age Aspect, *Histology and Embryology* 132 (1982) 29–35.
- [68] Q. Percy, M. Jeejo, M. Scholze, J. Tomlinson, J. Dressler, M. Zhang, J. Zwirner, Biomechanics of vascular areas of the human cranial dura mater, *J Mech Behav Biomed Mater* 125 (2022). <https://doi.org/10.1016/j.jmbbm.2021.104866>.
- [69] E. Zarzur, Mechanical Properties of the Human Lumbar Dura Mater, *Arq Neuropsiquiatr* 54 (1996) 455–460.
- [70] S. Cavelier, R.D. Quarrington, C.F. Jones, Mechanical properties of porcine spinal dura mater and pericranium, *J Mech Behav Biomed Mater* 126 (2022). <https://doi.org/10.1016/j.jmbbm.2021.105056>.
- [71] M. Evin, P. Sudres, P. Weber, Y. Godio-Raboutet, P.-J. Arnoux, E. Wagnac, Y. Petit, Y. Tillier, Experimental Bi-axial tensile tests of spinal meningeal tissues and constitutive models comparison, *Acta Biomater* 140 (2022) 446–456.

- [72] A. Sharma, E. Moore, L.N. Williams, An in vitro study of micromechanics, cellular proliferation and viability on both decellularized porcine dura grafts and native porcine dura grafts, *Biomedical Engineering Advances* 6 (2023) 100108. <https://doi.org/10.1016/j.bea.2023.100108>.
- [73] Y. Su, Z. Li, H. Zhu, J. He, B. Wei, D. Li, Electrohydrodynamic Fabrication of Triple-layered Polycaprolactone Dura Mater Substitute with Antibacterial and Enhanced Osteogenic Capability, *Chinese Journal of Mechanical Engineering: Additive Manufacturing Frontiers* 1 (2022) 100026. <https://doi.org/10.1016/j.cjmeam.2022.100026>.
- [74] A. Sharma, J. Liao, L.N. Williams, Structure and mechanics of native and decellularized porcine cranial dura mater, *Engineered Regeneration* 4 (2023) 205–213. <https://doi.org/10.1016/j.engreg.2023.02.004>.
- [75] J.A. Niestrawska, M. Rodewald, C. Schultz, E. Quansah, T. Meyer-Zedler, M. Schmitt, J. Popp, I. Tomasec, B. Ondruschka, N. Hammer, Morpho-mechanical mapping of human dura mater microstructure, *Acta Biomater* 170 (2023) 86–96. <https://doi.org/10.1016/j.actbio.2023.08.024>.
- [76] V.N. R., M. T.R.P., B. M.M., B. A.T., C.G. Montero, The Mechanical Properties of Human Dura Mater and the Effects of Storage Media, *Clin. Phys. Physiol. Meas* 2 (1981) 197–203.
- [77] D.R. Walsh, A.M. Ross, S. Malijauskaite, B.D. Flanagan, D.T. Newport, K.D. McGourty, J.J.E. Mulvihill, Regional mechanical and biochemical properties of the porcine cortical meninges, *Acta Biomater* 80 (2018) 237–246. <https://doi.org/10.1016/j.actbio.2018.09.004>.
- [78] J.T. Maikos, R.A.I. Elias, D.I. Shreiber, Mechanical properties of dura mater from the rat brain and spinal cord, *J Neurotrauma* 25 (2008) 38–51. <https://doi.org/10.1089/neu.2007.0348>.
- [79] C. Persson, S. Evans, R. Marsh, J.L. Summers, R.M. Hall, Poisson's ratio and strain rate dependency of the constitutive behavior of spinal dura mater, *Ann Biomed Eng* 38 (2010) 975–983. <https://doi.org/10.1007/s10439-010-9924-6>.
- [80] D. De Kegel, J. Vastmans, H. Fehervary, B. Depreitere, J. Vander Sloten, N. Famaey, Biomechanical characterization of human dura mater, *J Mech Behav Biomed Mater* 79 (2018) 122–134. <https://doi.org/10.1016/j.jmbbm.2017.12.023>.
- [81] N. Benko, E. Luke, Y. Alsanea, B. Coats, Mechanical characterization of the human pia-arachnoid complex, *J Mech Behav Biomed Mater* 120 (2021). <https://doi.org/10.1016/j.jmbbm.2021.104579>.
- [82] X. Jin, C. Ma, L. Zhang, K.H. Yang, A.I. King, G. Dong, J. Zhang, Biomechanical Response of the Bovine Pia-Arachnoid Complex to Normal Traction Loading at Varying Strain Rates, 2007.
- [83] X. Jin, K.H. Yang, A.I. King, Mechanical properties of bovine pia-arachnoid complex in shear, *J Biomech* 44 (2011) 467–474. <https://doi.org/10.1016/j.jbiomech.2010.09.035>.
- [84] X. Jin, H. Mao, K.H. Yang, A.I. King, Constitutive modeling of pia-arachnoid complex, *Ann Biomed Eng* 42 (2014) 812–821. <https://doi.org/10.1007/s10439-013-0948-6>.
- [85] X. Jin, J. Lee B., L. Leung Yee, L. Zhang, K. Yang H., A. King I., Biomechanical response of the Bovine Pia-Arachnoid Complex to Tensile Loading at Varying Strain-Rates, *Stapp Car Crash J* 50 (2006) 637–649. <https://doi.org/https://doi.org/10.4271/2006-22-0025>.

- [86] G. Fabris, Z. M. Suar, M. Kurt, Micromechanical heterogeneity of the rat pia-arachnoid complex, *Acta Biomater* 100 (2019) 29–37. <https://doi.org/10.1016/j.actbio.2019.09.044>.
- [87] N.L. Ramo, K.L. Troyer, C.M. Puttlitz, Viscoelasticity of spinal cord and meningeal tissues, *Acta Biomater* 75 (2018) 253–262. <https://doi.org/10.1016/j.actbio.2018.05.045>.
- [88] L. Qian, S. Wang, S. Zhou, Y. Sun, H. Zhao, Influence of pia-arachnoid complex on the indentation response of porcine brain at different length scales, *J Mech Behav Biomed Mater* 127 (2022). <https://doi.org/10.1016/j.jmbbm.2021.104925>.
- [89] J. Malda, J.C. de Grauw, K.E.M. Benders, M.J.L. Kik, C.H.A. van de Lest, L.B. Creemers, W.J.A. Dhert, P.R. van Weeren, Of Mice, Men and Elephants: The Relation between Articular Cartilage Thickness and Body Mass, *PLoS One* 8 (2013). <https://doi.org/10.1371/journal.pone.0057683>.
- [90] A.M. Corson, J. Laws, A. Laws, J.C. Litten, I.J. Lean, L. Clarke, Percentile growth charts for biomedical studies using a porcine model, *Animal* 2 (2008) 1795–1801. <https://doi.org/10.1017/S1751731108002966>.
- [91] H. Ozawa, T. Matsumoto, T. Ohashi, M. Sato, S. Kokubun, Mechanical properties and function of the spinal pia mater, 2004.
- [92] P. Sudres, M. Evin, E. Wagnac, N. Bailly, L. Diotalevi, A. Melot, P.-J. Arnoux, Y. Petit, Tensile mechanical properties of the cervical, thoracic and lumbar porcine spinal meninges, *J Mech Behav Biomed Mater* 115 (2021). <https://doi.org/https://doi.org/10.1016/j.jmbbm.2020.104280>.
- [93] A.R. Tunturi, Elasticity of the spinal cord, pia, and denticulate ligament in the dog, *J Neurosurg* 48 (1978) 975–979.
- [94] H. Kimpara, Y. Nakahira, M. Iwamoto, K. Miki, Investigation of Anteroposterior Head-Neck Responses during Severe Frontal Impacts Using a Brain-Spinal Cord Complex FE Model, *Stapp Car Crash J* 50 (2006) 509–544.
- [95] J.T. Maikos, R.A.I. Elias, D.I. Shreiber, Mechanical properties of dura mater from the rat brain and spinal cord, *J Neurotrauma* 25 (2008) 38–51. <https://doi.org/10.1089/neu.2007.0348>.
- [96] A. Tamura, W. Yano, D. Yoshimura, S. Nishikawa, Mechanical Characterization of Spinal Dura Mater Using a PD-Controlled Biaxial Tensile Tester, *J Mech Med Biol* 20 (2020). <https://doi.org/10.1142/S0219519420500232>.
- [97] D.R. Walsh, A.M. Ross, D.T. Newport, Z. Zhou, J. Kearns, C. Fearon, J. Lorigan, J.J.E. Mulvihill, Mechanical characterisation of the human dura mater, falx cerebri and superior sagittal sinus, *Acta Biomater* 134 (2021) 388–400. <https://doi.org/10.1016/j.actbio.2021.07.043>.
- [98] A. Tamura, S. Nishikawa, Effect of Anatomical Sites on the Mechanical Properties of Spinal Dura Subjected to Biaxial Stretching, *J Eng Sci Med Diagn Ther* 5 (2022). <https://doi.org/10.1115/1.4053341>.
- [99] A. Tamura, S. Nishikawa, DURAL MECHANICAL RESPONSES TO LOAD-CONTROLLED ASYMMETRIC BIAXIAL STRETCH, *J Mech Med Biol* 23 (2023). <https://doi.org/10.1142/S021951942350077X>.
- [100] A. Tamura, C. Sakaue, Effects of surface profile on porcine dural mechanical properties, *ClinicalBiomechanics* (2024).
- [101] J. Dobbing, The Later Growth of the Brain and its Vulnerability, *Pediatrics* 53 (1974). <http://publications.aap.org/pediatrics/article-pdf/53/1/2/942205/2.pdf>.

- [102] J. Dobbing, The Later Development of the Brain and its Vulnerability, *J Inherit Metab Dis* 5 (1982) 88.
- [103] J. Dickerson, J. Dobbing, Prenatal and postnatal growth and development of the central nervous system of the pig, *Proceedings of the Royal Society* 166 (1967) 384–395.
- [104] K.L. Thibault, S.S. Margulies, Material Properties of the Developing Porcine Brain, in: *International Research Council on Biomechanics of Injury*, 1996: pp. 75–85.
- [105] P. Saboori, Subarachnoid trabeculae, in: *Cerebrospinal Fluid and Subarachnoid Space: Clinical Anatomy and Physiology: Volume 1*, Elsevier, 2022: pp. 213–228.
<https://doi.org/10.1016/B978-0-12-819509-3.00006-7>.
- [106] P. Aïmediou, R. Grebe, Tensile strength of cranial pia mater: preliminary results, *J Neurosurg* (2004) 111–114.

Supplemental Information for

Mechanical Properties of the Meninges:

Large Language Model Augmented Systematic Review

Brandon P. Chelstrom, Maciej P. Polak, Dane Morgan, Corinne R. Henak

1) Validation of the LLM-based data extraction

Precision and recall were evaluated using ten sample studies. Briefly, property triplets from ten studies were manually extracted and assumed to be the ground truth. The sample studies were selected to target a search with the material as the *dura mater* and property of elastic modulus and varied with respect to publishing year (1960 to 2023), authors, journals, study type, study length, and relevance. Property triplets from ChatExtract were then compared to the ground truth where equivalent property triplets were defined as having identical units, identical values, and property text which uniquely describe the property (e.g. elastic modulus and Young's modulus would be equivalent, but elastic modulus and shear modulus would not). Precision and recall were calculated [1]:

$$Precision = \frac{TruePositives}{TruePositives + FalsePositives}$$

$$Recall = \frac{TruePositives}{TruePositives + FalseNegatives}$$

To establish the effect of LLM on the results on the semi-automatic review, the modified ChatExtract algorithm was run 10 times on two different LLMs (GPT-3.5-turbo and GPT-4o) for both a specific property value (elastic modulus) and a more general property value (stiffness) (Fig. S1). For the specific property of elastic modulus, GPT-4o had perfect recall with moderate precision indicating all correct property triplets were extracted with additional irrelevant property triplets. The inverse was true for the general property of stiffness: GPT-4o had perfect precision with moderate recall suggesting that while some property triplets were missed, all extracted property triplets were valid. GPT-3.5-turbo performed relatively the same for the specific and general property with

moderate recall and precision indicating some property triplets were not included while other irrelevant property triplets were included (Fig S1).

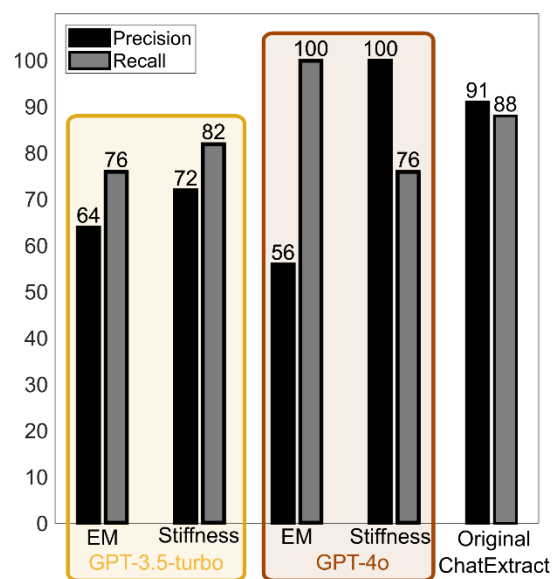


Fig S1: Precision and recall validation results from both GPT-3.5-turbo and GPT-4o for both specific (elastic modulus) and general (stiffness) properties compared to the original ChatExtract algorithm.

2) Additional Figures and Tables

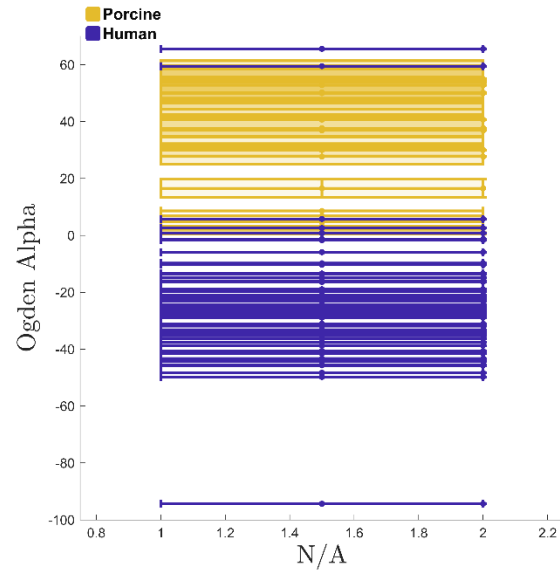


Fig S2: Distribution of Ogden exponents for human (purple) and porcine (orange) data. All values were standardized to the uniaxial incompressible form of $W = \frac{\mu}{\alpha^2} (\lambda_1^\alpha + \lambda_2^\alpha + \lambda_3^\alpha)$, where μ is the stiffness, α is the exponential term, and λ_i are the principal stretches.

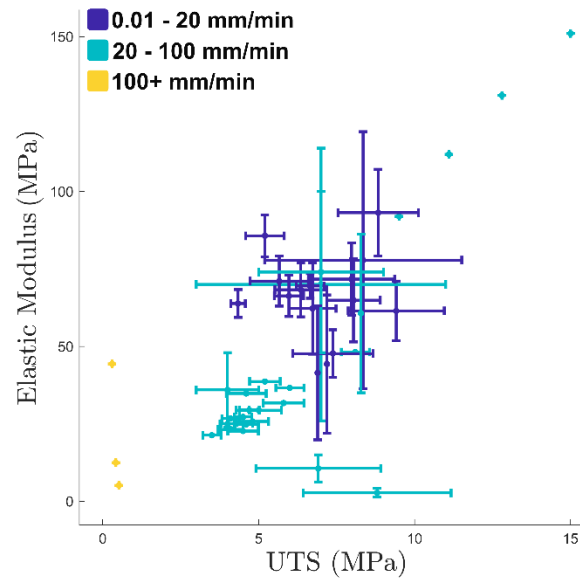


Fig S3: Ultimate tensile stress (UTS) versus elastic modulus for the *dura mater* at various loading rates. Plotted values are the average and standard deviation for various studies at various loading rates. Purple corresponds to slow loading rates ranging between 0.01 and 20 mm/min, green corresponds to moderate loading rates ranging between 20 and 100 mm/min, and yellow corresponds to fast loading rates above 100 mm/min.

Table S1: Relevant units for each property used for preprocessing of relevant sentences

Property	Relevant Units
Elastic Modulus	Pa, kPa, MPa, GPa
Young's Modulus	Pa, kPa, MPa, GPa
Shear Modulus	Pa, kPa, MPa, GPa
Relaxation Time	s, ms, μ s
Strain	-
Strain Rate	-
Rate Dependence	-
Stiffness	-

Nonlinear	-
Temperature	C, F, K
Linear Elastic	-
Viscoelastic	-
Pressure	-
Finite Element Parameter	-
Model	-

Table S2: Summary of dura mater mechanical papers, papers are arranged chronologically. N/R indicates that data were not reported in the reference, but atmospheric test conditions are assumed to be open to room when not reported. Post Mortem Time (PMT), Standard Deviation (SD).

Authors	DOI	Sample/ Cadaver Number	Cranial/ Spinal	Species	Location	Orientation	Treatment/ Study Purpose	Mean Age (SD) <range> [years]	Females /Males	PMT (SD) <range> [hours]	Sample Storage	Atmospheric Test Conditions	Sample Size (SD) <range> [mm]	Vascular/ Avascular	Loading Rate
(Galford and McElhaney, 1970) [2]	https://doi.org/10.1016/0021-9290(70)90007-2	11/2	Cranial	Human/ Monkey	N/R	N/R	Dynamic tissue properties	N/R	N/R	<6-12>	Maintained in ringer solution	Kept Moist with ringer solution	Rectangular, 63.5 mm x 6.35 mm	N/R	N/R
(Melvin et al., 1970) [3]	https://www.jstor.org/stable/44723768	36/-	Cranial	Human	N/R	Longitudinal, Transverse, Diagonal	Tissue orientation	N/R	N/R	3	Stored in saline solution	Open to Room	Dog Bone, Gage: 19.05 mm x 6.35 mm	N/R	0.061 s ⁻¹
(R. M. Kenedi, 1973) [4]	839107099	123/30	Cranial	Human	Parietal, Temporal, Frontal	N/R	Influence of strain rate	N/R	N/R	10	Stored in saline solution	Open to Room	Dog Bone, 19.05 mm x 6.35 mm	N/R	0.0666, 0.666, 6.66 s ⁻¹
(Van Noort et al., 1981a) [5]	https://doi.org/10.1016/0142-9612(81)90086-7	24/16	Cranial	Human	N/R	N/R	Half of samples preserved in glycerol	56 (16.5) <20 - 77>	N/R	<12-17>	Refrigerated saline	Open to Room	Rectangular, 40 mm x 5 mm	Avascular	50 mm/min
(Van Noort et al., 1981b) [6]	https://doi.org/10.1088/0143-0815/2/3/003	260/20	Cranial	Human	N/R	N/R	Some samples preserved in saline or glycerol	<28 - 88>	Both	<12-17>	Refrigerated saline	Open to Room	Rectangular, 60 mm x 5 mm, (Guage 40 mm x 5 mm)	Avascular	50 mm/min
(Zyablov et al., 1982) [7]	N/R	226/150	Cranial	Human	N/R	Longitudinal, transverse	Age effects on mechanics and physiology	<0.917 - 90>	N/R	N/R	N/R	Open to Room	Rectangular, 100 mm x 30 mm	N/R	0.016 N/min

(Kriewall et al., 1983) [8]	N/R	9/9	Cranial	Human	Parietal	Left, right	Mechanical behavior of fetal tissue	-0.136 (0.1) <-0.42 - 0>	5/4	N/R	Refrigerated at 5 or -10°C	Open to room (23C) but maintained in saline solution	Circular, 60 mm diameter	N/R	0.007 MPa/s
(McGarvey et al., 1984) [9]	https://doi.org/10.1016/0142-9612(84)90011-5	54/13	Cranial	Human	By sagittal sinus	Longitudinal, transverse	Half of samples preserved in glycerol	52 <17-72>	3/10	20	Maintained in Hanks balance solution (pH 7.4, osmolarity 310 mOs)	Maintained in Hanks solution at 37°C	Rectangular, 10.1 (0.2) mm x 7 mm	N/R	5, 50, 100, 500 %/min
(Tencer et al., 1985) [10]	https://doi.org/10.1097/0000-7632-198510000-00009	40/5	Spinal	Human	Posterior/ Anterior of lumbar, low thoracic, high thoracic, cervical	Longitudinal	Mechanical testing following spinal extension/fl exion	<N/R - 65>	N/R	N/R	Wrapped in wet towels at -20°C	Open to Room	Dog Bone, 38.1 mm x 2.54 mm	N/R	N/R
(Bylski et al., 1986) [11]	https://doi.org/10.1016/0021-9290(86)90105-3	11/7	Cranial	Human	Parietal/ Frontal	Left, right	Biaxial mechanical behavior of fetal tissue	-0.11 (0.096) <-0.286 - 0>	3/4	N/R	Refridated at 5 or frozen at -10°C	Open to room but maintained in saline solution	Circular, 40 mm diameter	N/R	0.02 mm/s
(Patin et al., 1993) [12]	https://doi.org/10.1213/0000-0539-199303000-00014	9/9	Spinal	Human/dog	Dorsal thoracolumbar	Longitudinal, transverse	Isotropy of spinal tissue	43.36 (29.22) <0.041-81>	3/6	N/R	Refrigerated in saline	Open to Room	Rectangular, 15 mm x 10 mm	N/R	100 mm/min
(Wolfenbarger et al., 1994) [13]	https://doi.org/10.1002/jab.770050313	95/10	Cranial	Human	Noted, but tested random	Noted, but tested random	Tissue freeze-dried prior to testing	40.3 (3.8) <17 - 51>	1/7	<2-3>	Freeze-dried, then stored on ice	Open to Room	Rectangular, 40 mm x 10 mm	N/R	10 mm/min
(Mickley et al., 1994) [14]	https://doi.org/10.1016/0031-9384(94)90384-0	97/-	Cranial	Rat	N/R	N/R	Thermal dose effect on surface temperature	N/R	N/R	0	N/R	In Situ	N/R	N/R	N/R
(E. Zarzur, 1996) [15]	https://doi.org/10.1590/S0004-282X1996000300015	6/3	Spinal	Human	Posterior lumbar	Longitudinal, transverse	Samples preserved in formalin	56.33 (17.55) <38 - 73>	-/3	72	Stored in formalin	Open to Room	Rectangular, 20 mm x 20 mm	N/R	20 mm/min
(Yamada et al., 1997) [16]	https://doi.org/10.3171/jns.1997.86.6.1012	15/15	Cranial	Human	N/R	N/R	Compare natural and synthetic mechanical behavior	30.7 (20.7) <3 62>	N/R	N/R	N/R	Open to room, sprayed with saline	Rectangular, 40 mm x 5 mm, (Gage 10 mm x 5 mm)	N/R	50 mm/min

(Sacks et al., 1998) [17]	https://doi.org/10.1115/1.2798027	90/5	Cranial	Human	Noted, but tested random	Parallel, perpendicular to fibers	Isotropy of cranial tissue, half subjected to allograft preparation	54 (22)	N/R	N/R	Frozen with saline in liquid nitrogen vapor	Submerged in room temperature saline	Rectangular, 20 mm x 4 mm)	N/R	50 mm/min
(Runza et al., 1999) [18]	https://doi.org/10.1213/00000539-199906000-00022	/6 (Human), /2 (Bovine)	Spinal	Human/Bovine	Dorsal lumbar (T12-L4/L5)	Longitudinal, transverse	PMT and storage temperature	58.5 <39 - 86>	3/3	2, 24, 120	Fresh, -4°C for 24 h, -4°C for 120 h, 4°C for 96 h	Open to room (20°C, 61% humidity)	Dog Bone, Gage: 22 mm x 4 mm	N/R	10 mm/min
(Wang et al., 2001) [19]	https://doi.org/10.1016/S0166-4328(00)00395-8	3/3	Cranial	Rat	Occipital	N/R	Dura cold probe temperature dispersion	N/R	N/R	0	N/R	In Situ	N/R	N/R	3 min
(Wilcox et al., 2003) [20]	https://doi.org/10.1007/s10776-003-0644-9	9/-	Spinal	Bovine	N/R	Longitudinal, transverse	Time-dependent and directional properties of spinal tissue	N/R	N/R	2	Frozen and thawed prior to testing	Submerged in saline (37°C)	Rectangular, 6-8 mm x 30-40 mm	N/R	0.03 - 0.13 s ⁻¹
(Bashkatov et al., 2003) [21]	https://doi.org/10.1016/S0006-3495(03)74750-X	N/R	Cranial	Human	N/R	N/R	Glucose and mannitol diffusion behavior	N/R	N/R	24	Stored at -12°C	Open to room (~20°C)	Rectangular, 10 mm x 10 mm	N/R	N/R
(Maikos et al., 2008) [22]	https://doi.org/10.1089/neu.2007.0348	23/- (Spinal), 16/- (Cranial)	Cranial/Spinal	Rat	Noted, but tested random	Longitudinal (Spinal)	Determine mechanical properties of rat dural tissue	0.21 (0.0136)	N/R	2	Stored in PBS	Open to room, but hydrated via ultrasonic humidifier	Rectangular, 12 mm x 1.5-2.5 mm	N/R	0.0014 or 19.4 s ⁻¹
(Persson et al., 2010) [23]	https://doi.org/10.1007/s10439-010-9924-6	38/20	Spinal	Bovine	Lumbar	Longitudinal, transverse	Evaluate nonlinear behavior of spinal tissue	<1.33 - 2>	N/R	N/R	Saline wrapped at -20°C	Open to room, but hydrated with saline solution	Dog Bone, 40 mm x 10 mm (Gage 10 mm x 4 mm)	N/R	15, 150, 1500 mm/min (0.01, 0.1, 1.0 s ⁻¹)
(Mazgajczyk et al., 2012) [24]	N/R	216/9	Spinal	Porcine	Cervical (C1-C7), ventral/dorsal	Longitudinal, transverse	Location and direction dependence of dura mater mechanical properties	N/R	N/R	24	Frozen, then prepped in 0.9% saline at 4°C	Open to room (24°C)	Rectangular, 8.1 (0.4) mm x 5.3 (0.3) mm	N/R	2 mm/min
(Shetye et al., 2014) [25]	https://doi.org/10.1016/j.jmbm.2014.02.014	12/4	Spinal	Ovine	Cervical (C1-C6)	Longitudinal, transverse	Biaxial characterization of fiber alignment	N/R	N/R	N/R	N/R	Open to Room	Rectangular 25 mm x 25 mm	N/R	N/R

(Ramo et al., 2018) [26]	https://doi.org/10.1155/1.4038261	45/4	Spinal	Ovine	Cervical (C2-C7)	Longitudinal	Characterize development of damage accumulation	N/R	N/R	N/R	Saline wrapped at -20°C	Saline bath at room temperature	Rectangular 20.81 (3.17) mm x 4.29 (0.9) mm	N/R	0.6, 60, 360 mm/min (0.0005, 0.051, 0.284 s ⁻¹)
(Walsh et al., 2018) [27]	https://doi.org/10.1016/j.actbio.2018.09.004	171/9	Cranial	Porcine	Frontal, temporal, parietal, occipital, sagittal sinus	Medial/Lateral, Rostral/Caudal	Biological, geometric, and location dependence of spinal tissue	0.583	N/R	48	Stored in PBS at 4°C	Open to room, but warmed to 37°C in PBS bath prior to testing	Rectangular, 20 mm x 2 mm (Frontal, occipital, parietal, temporal), 30 mm x 4 mm (Sagittal Sinus)	N/R	1 s ⁻¹
(Kegel et al., 2018) [28]	https://doi.org/10.1016/j.jmbbm.2017.12.023	53/5	Cranial	Human	Posterior, middle, anterior	Left, right	Extensive nonlinear mechanical characterization of spinal tissue	<68 - 88>	1/4	<96 - 144>	Dry-frozen at -18°C, thawed to 4°C	Open to Room	Rectangular, 10 mm x 10 mm	N/R	3.6 mm/min (1 s ⁻¹)
(Aydin et al., 2019) [29]	https://doi.org/10.340/jkns.2018.0130	28/7	Cranial	Human	Frontal	Left, right	Determine change of mechanical properties due to needle punctures	44.57 (11.58) <31 - 62>	4/3	30	Stored at -20°C, thawed at 4°C for 24 hrs, thawed at 20-25°C for 6 hours	Open to Room	Dog Bone, Gage 20 mm x 5 mm	N/R	10 m/min
(Zwirner et al., 2019a) [30]	https://doi.org/10.1038/s41598-019-52836-9	126/75	Cranial	Human	Temporal	Left, right	Influence of age, sex, and post mortem on mechanical properties	50 (23) <2 - 94>	25/48	75 (30) <11-146>	Cadavers stored at 4°C, samples frozen at -80°C	Open to Room	Dog Bone, Gage: 50 mm x 10 mm	N/R	20 mm/min
(Chengwei et al., 2019) [31]	https://doi.org/http://dx.doi.org/10.7507/1002-1892.201807085	-/5	Spinal	Ovine	Cervical (C6, C7), thoracic (T11, T12), lumbar (L4, L5)	Longitudinal, transverse	Investigate directional behavior of spinal tissue	1	-/5	N/R	Placed in saline	Open to room (25°C and 85% humidity)	Rectangular, 20 mm x 5 mm	N/R	0.96 mm/min
(Zwirner et al., 2019b) [32]	https://doi.org/10.1016/j.jmbbm.2019.04.035	36/18	Cranial	Human	N/R	N/R	Comparison between acellular and native tissue	48 <12-83>	6/12	71 (28) <14-121>	Samples frozen at -80°C	Open to Room	Dog Bone, Gage: 20 mm x 5 mm	N/R	20 mm/min
(Lipovka et al., 2020) [33]	https://doi.org/10.1088/1742-6596/1666/1/012062	3/3	Cranial	Human	N/R	N/R	Tissue harvested during microsurgical treatment method	N/R	N/R	<12 - 48>	Preserved in 0.9% saline at 2-5°C	Open to Room	Rectangular	N/R	2 mm/min

(Pierrat et al., 2020) [34]	https://doi.org/10.3389/fbioe.2020.00801	-/11	Cranial	Porcine	Parietal	Longitudinal, transverse	Nonlinear characterization for finite element models	0.432 (0.01) <0.423 - 0.442>	Mixed	<4 - 24>	Refrigerated in damp tissue	Open to room, but kept in saline solution prior to testing	Dog Bone, 63.5 mm x 3.2 mm	N/R	50 mm/min (0.01 s ⁻¹)
(Tamura et al., 2020) [35]	https://dx.doi.org/10.1142/S0219519420500232	18/6	Spinal	Porcine	Posterior thoracic and lumbar	Longitudinal, transverse	Verification of custom biaxial test device	N/R	N/R	24	Stored in saline at 4°C	Submerged in saline (37°C)	Rectangular, 15 mm x 15 mm	N/R	21 mm/min
(Walsh et al., 2021) [36]	https://doi.org/10.1016/j.actbio.2021.07.043	82/7	Cranial	Human	Frontal, parietal, temporal, occipital, falx cerebri, superior sagittal sinus	Medial/Lateral, Anterior/Posterior	Biaxial characterization of cranial tissue	<30-90>	1/6	N/R	Stored at -80°C with DMEM (1.8M) and sucrose (0.1M), warmed to 37°C in water bath, submerged in PBS at 4°C	Submerged in PBS bath (37°C)	Rectangular, 10 mm x 10 mm or 5 mm x 5 mm (Biaxial samples not sectioned)	N/R	N/R
(Su et al., 2022) [37]	https://doi.org/10.1016/j.cjmm.2022.100026	5/-	Cranial	Porcine	N/R	N/R	Fixed in 3.7% paraformaldehyde for 24 h at 4°C, dehydrated with alcohol aqueous solutions, and freeze-dried	N/R	N/R	24	Fixed in 3.7% paraformaldehyde for 24 h at 4°C, dehydrated with alcohol aqueous solutions, and freeze-dried	Open to Room	Rectangular, 50 mm x 6 mm	N/R	2 mm/min
(Pearcy et al., 2022) [38]	https://doi.org/10.1016/j.jmbbm.2021.104866	-/32	Cranial	Human	Temporal and parietal	Parallel and perpendicular to principal artery	Samples cross-embalmed prior to testing	81 (9) <58 - 95>	16/16	N/R	Samples preserved with crossadomix	Open to room (22°C)	Dog Bone, Gage 10 mm x 5 mm	Longitudinal and transverse to vasculature	20 mm/min
(Cavdar et al., 2022) [39]	https://doi.org/10.1016/j.wneu.2021.12.029	-/30	Cranial	Human	Frontal, parietal, temporal, occipital	Longitudinal (sagittal), transverse	Compare cortical thickness and histological measures	Female: 40.57 <27 - 63>, Males: 46.25 <32.58>	14/16	N/R	N/R	Open to Room	Rectangular, 30 mm x 10 mm	N/R	30 mm/min
(Cavelier et al., 2022) [40]	https://doi.org/10.1016/j.jmbbm.2021.105056	88/- (Spinal), 18/- (Cranial)	Spinal/Cranial	Porcine (landrace)	Dorsal and ventral cervical, thoracic, lumbar (Spinal), Frontal (Cranial)	Longitudinal, transverse	Compare directionality of cranial and spinal tissues	<0.25 - 0.33>	N/R	stored for <6 months, then 15	Wrapped in saline-soaked gauze at -20°C, defrosted for 15 h at 4°C, prepped in PBS	Continuous PBS flow at room temperature	Spinal Samples: Rectangular, 36 (2 mm x 5 (1 mm), Cranial Samples: Rectangular, 40 mm x 40 mm, Gage 16	N/R	15 mm/min

													(2) mm x 5 (1) mm		
(Evin et al., 2022) [41]	https://doi.org/10.1016/j.actbio.2021.11.028	31/8	Spinal	Porcine (landrace)	Cervical (C0-C7), Thoracic (T1-T15), Lumbar (L1-L5)	Longitudinal, transverse	Characterize spinal dura and pia for constitutive model development	<0.25 - 0.33>	N/R	12	Prepped in saline solution	Open to room, but hydrated with water droplets	Rectangular, 7 mm x 7 mm	N/R	3 mm/min
(Tamura et al., 2022) [42]	https://doi.org/10.1155/1.4053341	91/18	Spinal	Porcine	Dorsal and ventral cervical (C1-T1), thoracic (T2-T15), lumbar (L1-L5)	Longitudinal, transverse	Determine anatomical variation of spinal tissue	N/R	N/R	N/R	Stored in saline solution at 4°C	Floating in PBS bath at 37°C	Rectangular, 12 mm x 12 mm	N/R	12 mm/min
(Niestrawska et al., 2023) [43]	https://doi.org/10.1016/j.actbio.2023.08.024	90/6	Cranial	Human	Left ventral medial, lateral, medial, dorsal lateral, dorsal medial	Relative longitudinal, transverse	Link cranial microstructure heterogeneity to mechanical properties	78 (6) <70 - 87>	1/5	48	Frozen at -80°C, cooled to 4°C over 3 h	Submerged in PBS (pH = 7.4) bath (37°C)	Dog bone, Gage 20 mm x 5 mm	N/R	2 mm/min
(Sharma et al., 2023a) [44]	https://doi.org/10.1016/j.bea.2023.100108	8/6	Cranial	Porcine (Yorkshire)	N/R	N/R	Mechanical comparative native and decellularized tissue	<0.5 - 0.67>	-/6	2 (native), 76 (decellularized)	Freeze-dried in liquid nitrogen	Open to room, but sprayed with PBS	Circular, 14 mm diameter	N/R	0.6 mm/min
(Sharma et al., 2023b) [45]	https://doi.org/10.1016/j.engreg.2023.02.004	36/12 (uniaxial tension), 60/2 (microindentation)	Cranial	Porcine (Yorkshire)	Parietal (uniaxial tension), anterior, middle, posterior, left, and right (microindentation)	Longitudinal (anterior-posterior)	Mechanical comparative native and decellularized tissue	<0.5 - 0.67>	-/12	3	Samples kept in 1xPBS	Open to Room	Dog Bone, 40 mm x 10 mm (Gage 10 mm x 4 mm)	N/R	0.01 s ⁻¹ (uniaxial tension), 0.6 mm/min (microindentation)

(Zwirner et al., 2023) [46]	https://doi.org/10.1016/j.jmbbm.2022.105617	30/4	Cranial	Human	Occipital	Longitudinal	Evaluate rate dependence of dura mater, tissue fixed in PEG-Tris (pH = 7.4) at 4°C for 24 hrs	76 (6)	1/3	48	Cadavers stored at 4°C, samples frozen at -80°C	Open to room (22°C)	Dog bone, Gage: 20 mm x 5 mm	N/R	18000, 30000, 42000 mm/min (15, 25, 35 s ⁻¹)
(A. Tamura et al., 2023) [47]	https://doi.org/10.1142/S021951942350077X	26/10	Spinal	Porcine	Lumbar	Longitudinal, transverse	Compared spinal samples with and without elastase treatment	N/R	N/R	24	Stored in saline solution at 4°C	Open to Room	Rectangular, 12 mm x 12 mm	N/R	12 mm/min
(Tamura and Sakaue, 2024) [48]	https://doi.org/10.1016/j.clinbiomech.2024.106189	55/10	Spinal	Porcine	Cervical, lumbar	Longitudinal, transverse	Determine effect of surface roughness on mechanics	N/R	N/R	48	mounted on agar gel (1:25 mixing weight), submerged in PBS at 4°C	Sample covered with windshield at room temperature (~22°C)	Rectangular, 12 mm x 12 mm	N/R	0.9 mm/min

Table S3: Summary of arachnoid mater mechanical papers and pia-arachnoid complex (PAC) papers, papers are arranged chronologically. N/R indicates that data were not reported in the reference, but atmospheric test conditions are assumed to be open to room when not reported.

Authors	DOI	Sample/ Cadaver Number	Cranial/ Spinal	Species	Location	Orientation	Treatment/ Study Purpose	Mean Age (SD) <range> [years]	Females/ Males	PMT (SD) <range> [hours]	Sample Storage	Atmospheric Test Conditions	Sample Size (SD) <range> [mm]	Vascular/ Avascular	Loading Rate
(Jin et al., 2006) [49]	https://doi.org/10.4271/2006-22-0025	40/10	Cranial	Bovine	Dorsal	Longitudinal (sagittal), transverse (coronal)	Mechanically characterize the cranial PAC in tension	<0.327 - 0.385>	N/R	48	Stored in artificial cerebral spinal fluid	Open to room, but sprayed with artificial cerebral spinal fluid	Rectangular, 65 mm x 30 mm, (Gage 20 mm x 25.6 mm)	N/R	60, 600, 6000, 120000 mm/min (0.05, 0.5, 5, 100 s ⁻¹)
(Jin et al., 2007) [50]	https://doi.org/10.4271/2007-22-0004	40/-	Cranial	Bovine	Frontal, occipital, parietal	N/R	Mechanically characterize the cranial PAC in traction	<0.327 - 0.385>	N/R	48	Soaked in artificial cerebral spinal fluid	Open to room, but sprayed with artificial cerebral spinal fluid	Rectangular, 12.7 mm x 12.7 mm	N/A	0.516, 2.82, 28.8, 165 mm/min (0.36, 2.0, 20.5, 116.3 s ⁻¹)

(Jin et al., 2011) [51]	https://doi.org/10.1016/j.jbiomech.2010.09.035	43/4	Cranial	Bovine	Frontal, occipital, parietal	N/R	Mechanically characterize the cranial PAC in shear	<0.327 - 0.385>	N/R	48	Soaked in artificial cerebral spinal fluid	Open to room (20°C), but sprayed with artificial cerebral spinal fluid	Rectangular, 12.7 mm x 12.7 mm	N/R	1.2, 10.2, 102 mm/min (0.84, 7.3, 72 s ⁻¹)
(Jin et al., 2014) [52]	https://doi.org/10.1007/s10439-013-0948-6	N/R	Cranial	Bovine	N/R	N/R	Develop constitutive equations for the macroscopic cranial PAC	<0.327 - 0.385>	N/R	48	Soaked in artificial cerebral spinal fluid	Open to room (20°C), but sprayed with artificial cerebral spinal fluid	Rectangular, 12.7 mm x 12.7 mm (normal traction and shear), Rectangular, Gauge 20 mm x 25.6 mm (Uniaxial tension)	N/R	0.05, 0.5, 5, 100 s ⁻¹
(Ramo et al., 2018) [53]	https://doi.org/10.1016/j.actbio.2018.05.045	8/8	Spinal	Ovine	Cervical (C0-C7)	Longitudinal	PAC tested following full cord testing	<4 - N/R>	8/-	5	Soaked in saline solution in airtight container	Open to room	Rectangular, 60 mm x 10 mm	N/R	0.016, 0.16, 1.6, 16.0 s ⁻¹
(Fabris et al., 2019) [54]	https://doi.org/10.1016/j.actbio.2019.09.044	18/12	Cranial	Rat (Sprague-Dawley)	Cortical, cerebellar	N/R	Determine effects of vasculature on PAC properties	<0.154 - 0.231>	-/12	0.33	Soaked in PBS	Sample immersed in PBS	Rectangular, grid of 99 points in a 90 µm x 90 µm area	Noted by AFM and immunofluorescence	0.6 - 3 mm/min (0.33 - 1.66 s ⁻¹)
(Benko et al., 2021) [55]	https://doi.org/10.1016/j.jmbb.2021.104579	109/5	Cranial	Human	Superior and inferior regions of the frontal, occipital, parietal	N/R	Determine traction modulus of individual arachnoid trabeculae	60 (19.2) <32 - 81>	2/3	56	Frozen and defrosted over 2 days to room temperature, Inflated with Saline	In Situ	Tissue not sectioned, scan volume of 5 mm x 5 mm x 1.64 mm	N/R	0.00159 MPa/min
(Qian et al., 2022) [56]	https://doi.org/10.1016/j.jmbb.2021.104925	-/32	Cranial	Porcine	N/R	Left/Right pooled	Determine mechanical behavior of PAC across length scales	0.5	N/R	6	Cortex submerged in artificial cerebral spinal fluid	Sample immersed in artificial cerebral spinal fluid at room temperature	N/R	N/R	48 and 96 mm/min (0.64 and 1.27 s ⁻¹)

Table S4: Summary of pia mater mechanical papers and, papers are arranged chronologically. N/R indicates that data were not reported in the reference, but atmospheric test conditions are assumed to be open to room when not reported.

Authors	DOI	Sample/ Cadaver Number	Cranial/ Spinal	Species	Location	Orientation	Treatment/ Study Purpose	Mean Age (SE) <range> [years]	Females/ Males	PMT (SE) <range> [hours]	Sample Storage	Atmospheric Test Conditions	Sample Size (SE) <range> [mm]	Vascular/ Avascular	Loading Rate
(A. Tunturi, 1978) [57]	https://doi.org/10.3171/jns.1978.48.6.0975	N/R	Spinal	Dog	Thoracic (T9 - T11)	Longitudinal	Determine static mechanical properties of the spinal cord	N/R	N/R	1	Sprayed with ringer solution	Sprayed with ringer solution	Rectangular, 40 mm x - mm	N/R	0.049 N/min
(Ozawa, 2004) [58]	https://doi.org/10.3171/spi.2004.41.1.0122	18/9	Spinal	Rabbit	Cervical (C5 - C6)	Transverse	Determine influence of pia mater spine mechanical properties	N/R	N/R	0.5	Stored in saline solution at room temperature (16°C)	Open to Room	Whole spinal column, 10 mm x 3 mm	N/R	0.012 N/min
(Aimedieu & Grebe, 2004) [59]	https://doi.org/10.3171/jns.2004.100.1.0111	9/6	Cranial	Bovine	Posterior	Right hemisphere	Determine the elastic properties of cranial pia mater	0.865 (0.54)	N/R	<6 - 16>	Cortex submerged in 0.9% saline solution at 4°C	Submerged in water bath (37°C)	Rectangular, 95 mm x 35 mm	N/R	0.5 mm/min
(Kimpara et al., 2006) [60]	https://doi.org/10.4271/2006-22-0019	52/6	Spinal	Porcine	By denticulate ligament, posterior median septum, posterolateral sulcus	N/R	Determine localized mechanical properties of the spinal pia mater	N/R	N/R	5	Open to room (24°C) at >50% humidity	Open to room (24°C) at >50% humidity	Rectangular, 20 mm x 1 mm	N/R	0.005, 0.05, 0.5 s ⁻¹
(Li et al., 2020) [61]	https://doi.org/10.1016/j.clinbiomech.2020.105108	48/20	Cranial	Ovine	Left/Right Hemisphere sagittal sinus	N/R	Determine viscoelastic properties of cranial pia mater at different loading rates	<0.461 - 0.538>	N/R	6	Cortex transferred in 4°C, and prepped at room temperature (22°C), maintained in 0.9% saline solution	Open to room (22°C)	Rectangular, 20 mm x 3-5 mm (Gage 10 mm x 4 mm)	N/R	1, 5, 10, 30, 100, 300, 500 mm/min (0.00167, 0.0083, 0.0167, 0.05, 0.083, 0.16, 0.5, 0.83 s ⁻¹)

(Sudres et al., 2021) [62]	https://doi.org/10.1016/j.jmbb.2020.104280	47/6	Spinal	Porcine (Yorkshire x Landrace)	Cervical (C1 - T1), thoracic (T1 - T4), lumbar (T14 - L6)	Longitudinal	Mechanical characterization of the pia mater	<0.167 - 0.250>	2/4	12.5	Stored in PBS at 4°C	Open to Room (20°C)	Rectangular, 10.35 (1.98) mm x 9.82 (3.31) mm	N/R	12 mm/min
(Evin et al., 2022) [41]	https://doi.org/10.1016/j.actbio.2021.11028	31/8	Spinal	Porcine (landrace)	Cervical (C0-C7), Thoracic (T1-T15), Lumbar (L1-L5)	Longitudinal, transverse	Characterize spinal dura and pia for constitutive model development	<0.25 - 0.33>	N/R	12	Prepped in saline solution	Open to room, but hydrated with water droplets	Rectangular, 7 mm x 7 mm	N/R	3 mm/min

References

- [1] M.P. Polak, D. Morgan, Extracting Accurate Materials Data from Research Papers with Conversational Language Models and Prompt Engineering, (2023). <http://arxiv.org/abs/2303.05352>.
- [2] J.E. Galford, J.H. McElhaney, A viscoelastic study of scalp, brain, and dura, *J Biomech* 3 (1970) 211–221. [https://doi.org/10.1016/0021-9290\(70\)90007-2](https://doi.org/10.1016/0021-9290(70)90007-2).
- [3] J.W. Melvin, J.H. McElhaney, V.L. Roberts, Development of a Mechanical Model of the Human Head — Determination of Tissue Properties and Synthetic Substitute Materials, *SAE Transactions* 79 (1970) 2685–2694. <https://about.jstor.org/terms>.
- [4] R.M.. Kenedi, Perspectives in Biomedical Engineering, in: R.M.. Kenedi (Ed.), *Biological Engineering Society*, University Park Press, 1973: pp. 215–222.
- [5] R. Van Noort, M.M. Black, T.R.P. Martin, S. Meanley, A study of the uniaxial mechanical properties of human dura mater preserved in glycerol, *Biomaterials* 2 (1981) 41–45.
- [6] R. Van Noort, T.R.P. Martin, M.M. Black, A.T. Barker, C.G. Montero, The mechanical properties of human dura mater and the effects of storage media, *Clin. Phys. Physiol. Meas* 2 (1981) 197–203. <https://doi.org/https://doi.org/10.1088/0143-0815/2/3/003>.
- [7] V.I. Zyablov, Y.N. Shapovalov, K.D. Toskin, V. V Tkach, V. V Zhebrovsky, L.S. Georgievskaya, Structure and Physical-Mechanical Properties of the Human Dural Mind in the Age Aspect, *Histology and Embryology* 132 (1982) 29–35.
- [8] T.J. Kriewall, N. Akkas, D.I. Bylski, B. Program, J.W. Melvin, Mechanical Behavior of Fetal Dura Mater Under Large Axisymmetric Inflation, 1983. http://asmedigitalcollection.asme.org/biomechanical/article-pdf/105/1/71/5481347/71_1.pdf.
- [9] K. Mcgarvey A., J. Micheal Lee, D. Boughner R., Mechanical Suitability of Glycerol-Preserved Human Dura Mater for Construction of Prosthetic Cardiac Valves, *Biomaterials* 5 (1984) 109–117. [https://doi.org/10.1016/0142-9612\(84\)90011-5](https://doi.org/10.1016/0142-9612(84)90011-5).
- [10] T. A.F., A. B.L., R.L. Ferguson, A Biomechanical Study of Thoracolumbar Spine Fractures with Bone in the Canal. Part III. Mechanical Properties of the Dura and Its Tethering Ligaments, *Spine (Phila Pa 1976)* 10 (1985) 741–747.

- [11] D.I. Bylski, T.J. Kriewall, N. Akkas, J.W. Melvin, Mechanical Behavior of Fetal Dura Mater Under Large Deformation Biaxial Tension, *J Biomech* 19 (1986) 19–26. [https://doi.org/https://doi.org/10.1016/0021-9290\(86\)90105-3](https://doi.org/https://doi.org/10.1016/0021-9290(86)90105-3).
- [12] D.J. Patin, E.C. Eckstein, K. Harum, V.S. Pallares, Anatomic and Biomechanical Properties of Human Lumbar Dura Mater, *Anesth Analg* 76 (1993) 535–540. <https://doi.org/10.1213/00000539-199303000-00014>.
- [13] L. Wolfinbarger, Y. Zhang, B.L.T. Adam, D. Homsy, K. Gates, V. Sutherland, Biomechanical aspects on rehydrated freeze-dried human allograft dura mater tissues, *Journal of Applied Biomaterials* 5 (1994) 265–270. <https://doi.org/10.1002/jab.770050313>.
- [14] A. Mickley G., B. Cobb L., P. Mason A., S. Farrell, Disruption of a Putative Working Memory Task and Selective Expression of Brain c-fos Following Microwave-Induced Hyperthermia, *Physiol Behav* 44 (1994) 1029–1038.
- [15] E. Zarzur, Mechanical Properties of the Human Lumbar Dura Mater, *Arq Neuropsiquiatr* 54 (1996) 455–460.
- [16] K. Yamada, S. Miyamoto, I. Nagata, H. Kikuchi, Y. Ikada, H. Iwata, K. Yamamoto, Development of a dural substitute from synthetic bioabsorbable polymers, *J Neurosurg* 86 (1997) 1012–1017.
- [17] M.S. Sacks, J. Hamann, S.E. Otano-Lata, T.I. Malinin, Local Mechanical Anisotropy in Human Cranial Dura Mater Allografts, *J Biomech Eng* 120 (1998) 541–544. http://asmedigitalcollection.asme.org/biomechanical/article-pdf/120/4/541/5767037/541_1.pdf.
- [18] M. Runza, R. Pietrabissa, S. Mantero, A. Albani, V. Quaglini, R. Contro, Lumbar Dura Mater Biomechanics: Experimental Characterization and Scanning Electron Microscopy Observations, *Anesth Analg* 88 (1999) 1317–1321.
- [19] W. Yuan, C. Kathleen C., The role of the dura in conditioned taste avoidance induced by cooling the area postrema of male rats, *Behavioural Brain Research* 122 (2001) 113–129. [https://doi.org/https://doi.org/10.1016/S0166-4328\(00\)00395-8](https://doi.org/https://doi.org/10.1016/S0166-4328(00)00395-8).
- [20] R.K. Wilcox, L.E. Bilston, D.C. Barton, R.M. Hall, Mathematical model for the viscoelastic properties of dura mater, in: *J Orthop Sci*, 2003: pp. 432–434.
- [21] A. Bashkatov N., E. Genina A., Y. Sinichkin P., V. Kochubey I., N. Lakodina A., V. Tuchin V., Glucose and Mannitol Diffusion in Human Dura Mater, *Biophys J* 85 (2003) 3310–3318.
- [22] J.T. Maikos, R.A.I. Elias, D.I. Shreiber, Mechanical properties of dura mater from the rat brain and spinal cord, *J Neurotrauma* 25 (2008) 38–51. <https://doi.org/10.1089/neu.2007.0348>.
- [23] C. Persson, S. Evans, R. Marsh, J.L. Summers, R.M. Hall, Poisson’s ratio and strain rate dependency of the constitutive behavior of spinal dura mater, *Ann Biomed Eng* 38 (2010) 975–983. <https://doi.org/10.1007/s10439-010-9924-6>.
- [24] E. Mazgajczyk, K. Scigala, M. Czy, W. Jarmundowicz, R. BedZinski, Mechanical Properties of Cervical Dura Mater, *Acta of Bioengineering and Biomaterials* 14 (2012) 51–58.
- [25] S. Shetye S., M. Deault M., C. Puttlitz M., Biaxial response of ovine spinal cord dura mater, *J Mech Behav Biomed Mater* 34 (2014) 146–153. [10.1016/j.jmbbm.2014.02.014](https://doi.org/10.1016/j.jmbbm.2014.02.014) (accessed July 7, 2024).
- [26] N. Ramo, S.S. Shetye, C.M. Puttlitz, Damage Accumulation Modeling and Rate Dependency of Spinal Dura Mater, *J Eng Sci Med Diagn Ther* 1 (2018). <https://doi.org/10.1115/1.4038261>.

- [27] D.R. Walsh, A.M. Ross, S. Malijauskaite, B.D. Flanagan, D.T. Newport, K.D. McGourty, J.J.E. Mulvihill, Regional mechanical and biochemical properties of the porcine cortical meninges, *Acta Biomater* 80 (2018) 237–246. <https://doi.org/10.1016/j.actbio.2018.09.004>.
- [28] D. De Kegel, J. Vastmans, H. Fehervary, B. Depreitere, J. Vander Sloten, N. Famaey, Biomechanical characterization of human dura mater, *J Mech Behav Biomed Mater* 79 (2018) 122–134. <https://doi.org/10.1016/j.jmbbm.2017.12.023>.
- [29] H.E. Aydın, C. Kızmazoglu, I. Kaya, B. Husemoglu, G. Sozer, H. Havıtcıoglu, A. Arslantas, Biomechanical properties of the cranial dura mater with puncture defects: An In Vitro study, *J Korean Neurosurg Soc* 62 (2019) 382–388. <https://doi.org/10.3340/jkns.2018.0130>.
- [30] J. Zwirner, M. Scholze, J.N. Waddell, B. Ondruschka, N. Hammer, Mechanical Properties of Human Dura Mater in Tension – An Analysis at an Age Range of 2 to 94 Years, *Sci Rep* 9 (2019). <https://doi.org/10.1038/s41598-019-52836-9>.
- [31] C. Yang, X. Yang, X. Lan, H. Zhang, M. Wang, Y. Zhang, Y. Xu, P. Zhen, Structure and mechanical characteristics of spinal dura mater in different segments of sheep’s spine, *Chinese Journal of Reparative and Reconstructive Surgery* 33 (2019) 232–238. <https://doi.org/10.7507/1002-1892.201807085>.
- [32] J. Zwirner, B. Ondruschka, M. Scholze, G. Schulze-Tanzil, N. Hammer, Mechanical and morphological description of human acellular dura mater as a scaffold for surgical reconstruction, *J Mech Behav Biomed Mater* 96 (2019) 38–44. <https://doi.org/10.1016/j.jmbbm.2019.04.035>.
- [33] A.I. Lipovka, A. V. Dubovoy, D. V. Parshin, The study of the strength properties of the human dura mater: The experience of one research center, in: *J Phys Conf Ser*, IOP Publishing Ltd, 2020. <https://doi.org/10.1088/1742-6596/1666/1/012062>.
- [34] B. Pierrat, L. Carroll, F. Merle, D.B. MacManus, R. Gaul, C. Lally, M.D. Gilchrist, A. Ní Annaidh, Mechanical Characterization and Modeling of the Porcine Cerebral Meninges, *Front Bioeng Biotechnol* 8 (2020). <https://doi.org/10.3389/fbioe.2020.00801>.
- [35] A. Tamura, W. Yano, D. Yoshimura, S. Nishikawa, Mechanical Characterization of Spinal Dura Mater Using a PD-Controlled Biaxial Tensile Tester, *J Mech Med Biol* 20 (2020). <https://doi.org/10.1142/S0219519420500232>.
- [36] D.R. Walsh, A.M. Ross, D.T. Newport, Z. Zhou, J. Kearns, C. Fearon, J. Lorigan, J.J.E. Mulvihill, Mechanical characterisation of the human dura mater, falx cerebri and superior sagittal sinus, *Acta Biomater* 134 (2021) 388–400. <https://doi.org/10.1016/j.actbio.2021.07.043>.
- [37] Y. Su, Z. Li, H. Zhu, J. He, B. Wei, D. Li, Electrohydrodynamic Fabrication of Triple-layered Polycaprolactone Dura Mater Substitute with Antibacterial and Enhanced Osteogenic Capability, *Chinese Journal of Mechanical Engineering: Additive Manufacturing Frontiers* 1 (2022) 100026. <https://doi.org/10.1016/j.cjmeam.2022.100026>.
- [38] Q. Pearcy, M. Jeejo, M. Scholze, J. Tomlinson, J. Dressler, M. Zhang, J. Zwirner, Biomechanics of vascular areas of the human cranial dura mater, *J Mech Behav Biomed Mater* 125 (2022). <https://doi.org/10.1016/j.jmbbm.2021.104866>.
- [39] S. Çavdar, S. Sürücü, M. Özkan, B. Köse, A.N. Malik, E. Aydoğmuş, Ö. Tanış, İ. Lazoğlu, Comparison of the Morphologic and Mechanical Features of Human Cranial Dura and Other Graft Materials Used for Duraplasty, *World Neurosurg* 159 (2022) e199–e207.

- [40] S. Cavelier, R.D. Quarrington, C.F. Jones, Mechanical properties of porcine spinal dura mater and pericranium, *J Mech Behav Biomed Mater* 126 (2022). <https://doi.org/10.1016/j.jmbbm.2021.105056>.
- [41] M. Evin, P. Sudres, P. Weber, Y. Godio-Raboutet, P.-J. Arnoux, E. Wagnac, Y. Petit, Y. Tillier, Experimental Bi-axial tensile tests of spinal meningeal tissues and constitutive models comparison, *Acta Biomater* 140 (2022) 446–456.
- [42] A. Tamura, S. Nishikawa, Effect of Anatomical Sites on the Mechanical Properties of Spinal Dura Subjected to Biaxial Stretching, *J Eng Sci Med Diagn Ther* 5 (2022). <https://doi.org/10.1115/1.4053341>.
- [43] J.A. Niestrawska, M. Rodewald, C. Schultz, E. Quansah, T. Meyer-Zedler, M. Schmitt, J. Popp, I. Tomasec, B. Ondruschka, N. Hammer, Morpho-mechanical mapping of human dura mater microstructure, *Acta Biomater* 170 (2023) 86–96. <https://doi.org/10.1016/j.actbio.2023.08.024>.
- [44] A. Sharma, J. Liao, L.N. Williams, Structure and mechanics of native and decellularized porcine cranial dura mater, *Engineered Regeneration* 4 (2023) 205–213. <https://doi.org/10.1016/j.engreg.2023.02.004>.
- [45] A. Sharma, E. Moore, L.N. Williams, An in vitro study of micromechanics, cellular proliferation and viability on both decellularized porcine dura grafts and native porcine dura grafts, *Biomedical Engineering Advances* 6 (2023) 100108. <https://doi.org/10.1016/j.bea.2023.100108>.
- [46] J. Zwirner, B. Ondruschka, M. Scholze, A. Thambyah, J. Workman, N. Hammer, J.A. Niestrawska, Dynamic load response of human dura mater at different velocities, *J Mech Behav Biomed Mater* 138 (2023). <https://doi.org/10.1016/j.jmbbm.2022.105617>.
- [47] A. Tamura, S. Nishikawa, Dural Mechanical Responses to Load-Controlled Asymmetric Biaxial Stretch, *J Mech Med Biol* 23 (2023). <https://doi.org/10.1142/S021951942350077X>.
- [48] A. Tamura, C. Sakaue, Effects of surface profile on porcine dural mechanical properties, *Clinical Biomechanics* (2024).
- [49] X. Jin, J. Lee B., L. Leung Yee, L. Zhang, K. Yang H., A. King I., Biomechanical response of the Bovine Pia-Arachnoid Complex to Tensile Loading at Varying Strain-Rates, *Stapp Car Crash J* 50 (2006) 637–649. <https://doi.org/https://doi.org/10.4271/2006-22-0025>.
- [50] X. Jin, C. Ma, L. Zhang, K.H. Yang, A.I. King, G. Dong, J. Zhang, Biomechanical Response of the Bovine Pia-Arachnoid Complex to Normal Traction Loading at Varying Strain Rates, 2007.
- [51] X. Jin, K.H. Yang, A.I. King, Mechanical properties of bovine pia-arachnoid complex in shear, *J Biomech* 44 (2011) 467–474. <https://doi.org/10.1016/j.jbiomech.2010.09.035>.
- [52] X. Jin, H. Mao, K.H. Yang, A.I. King, Constitutive modeling of pia-arachnoid complex, *Ann Biomed Eng* 42 (2014) 812–821. <https://doi.org/10.1007/s10439-013-0948-6>.
- [53] N.L. Ramo, K.L. Troyer, C.M. Puttlitz, Viscoelasticity of spinal cord and meningeal tissues, *Acta Biomater* 75 (2018) 253–262. <https://doi.org/10.1016/j.actbio.2018.05.045>.
- [54] G. Fabris, Z. M. Suar, M. Kurt, Micromechanical heterogeneity of the rat pia-arachnoid complex, *Acta Biomater* 100 (2019) 29–37. <https://doi.org/10.1016/j.actbio.2019.09.044>.
- [55] N. Benko, E. Luke, Y. Alsanea, B. Coats, Mechanical characterization of the human pia-arachnoid complex, *J Mech Behav Biomed Mater* 120 (2021). <https://doi.org/10.1016/j.jmbbm.2021.104579>.

- [56] L. Qian, S. Wang, S. Zhou, Y. Sun, H. Zhao, Influence of pia-arachnoid complex on the indentation response of porcine brain at different length scales, *J Mech Behav Biomed Mater* 127 (2022). <https://doi.org/10.1016/j.jmbbm.2021.104925>.
- [57] A.R. Tunturi, Elasticity of the spinal cord, pia, and denticulate ligament in the dog, *J Neurosurg* 48 (1978) 975–979.
- [58] H. Ozawa, T. Matsumoto, T. Ohashi, M. Sato, S. Kokubun, Mechanical properties and function of the spinal pia mater, 2004.
- [59] P. Aimedieu, R. Grebe, Tensile strength of cranial pia mater: preliminary results, *J Neurosurg* 100 (2004) 111–114.
- [60] H. Kimpara, Y. Nakahira, M. Iwamoto, K. Miki, Investigation of Anteroposterior Head-Neck Responses during Severe Frontal Impacts Using a Brain-Spinal Cord Complex FE Model, *Stapp Car Crash J* 50 (2006) 509–544.
- [61] Y. Li, W. Zhang, Y.C. Lu, C.W. Wu, Hyper-viscoelastic mechanical behavior of cranial pia mater in tension, *Clinical Biomechanics* 80 (2020). <https://doi.org/10.1016/j.clinbiomech.2020.105108>.
- [62] P. Sudres, M. Evin, E. Wagnac, N. Bailly, L. Diotalevi, A. Melot, P.-J. Arnoux, Y. Petit, Tensile mechanical properties of the cervical, thoracic and lumbar porcine spinal meninges, *J Mech Behav Biomed Mater* 115 (2021). <https://doi.org/https://doi.org/10.1016/j.jmbbm.2020.104280>.